Université de Montréal

Modélisation et détermination des paramètres pharmacocinétiques du trans-resvératrol par voie topique chez le lapin et prédiction de la pharmacocinétique chez l'humain

par

Anna Maria Schinas, B.Sc.

Faculté de pharmacie

Mémoire présenté à la Faculté des études supérieures
en vue de l'obtention du grade de
Maître ès sciences (M.Sc.)
en sciences pharmaceutiques
option pharmacologie

Décembre 2005

Université de Montréal
Faculté des études supérieures

Ce mémoire intitulé :

Modélisation et détermination des paramètres pharmacocinétiques du trans-resvératrol par voie topique chez le lapin et prédiction de la pharmacocinétique chez l'humain

Présentée par :

Anna Maria Schinas, B.Sc.

Comité de mémoire :

Murray P. Ducharme, Pharm.D., FCCP, FCP
Jacques Turgeon, B.Sc. Pharm., Ph.D.
Tristan Booth, Ph.D., Cchem MRSC,
Chef de la direction Scientifique, Royalmount Pharma

Ce mémoire a été évalué par un jury composé des personnes suivantes :

France Varin, B.Pharm, Ph.D.
professeur titulaire
président-rapporteur

Murray P. Ducharme, Pharm.D., FCCP, FCP
professeur associé et
vice-président PK/PD Services Pharma MDS
directeur de recherche

Jacques Turgeon, B.Sc. Pharm., Ph.D.
doyen et professeur titulaire
co-directeur de recherche

Fahima Nekka, Ph.D.
professeure adjointe
membre du jury

RÉSUMÉ

Le resvératrol (3,4',5-trihydroxystilbène) est un phytoalexine synthétisé par certaines plantes suite à une infection fongique ou une irradiation aux rayons ultraviolets. Le resvératrol existe sous deux formes, soient les isomères *cis*- et *trans*-resvératrol. Parmi sa vaste gamme d'effets thérapeutiques potentiels, le *trans*-resvératrol semble inhiber la réplication du virus de l'herpès simplex (HSV), ce qui pourrait potentiellement en faire un traitement efficace contre les infections chroniques d'herpès. Le premier objectif de ce mémoire était de caractériser la pharmacocinétique du *trans*-resvératrol chez les lapins, suite à l'application topique de deux crèmes contenant du *trans*-resvératrol. Le second objectif était de prédire par allométrie la dose topique à administrer chez l'humain.

Les concentrations plasmatiques observées de *trans*-resvératrol après l'application des deux crèmes indique que le *trans*-resvératrol diffuse à travers les différentes couches de la peau jusqu'a l'épiderme basal, là où la réplication du virus de l'herpès a lieu. Au total, 24 lapins ont reçu des doses topiques multiples de crème contenant 12.5% ou 19.0% de *trans*-resvératrol pendant 28 jours consécutifs. Des analyses pharmacocinétiques noncompartimentales et compartimentales ont été réalisées à partir des concentrations plasmatiques de *trans*-resvératrol. L'analyse compartimentale a été faite avec le logiciel Adapt II® pour l'analyse individuelle et avec IT2S® pour les analyses de population. La biodisponibilité relative des deux formulations a été évaluée avec les paramètres pharmacocinétiques obtenus par les méthodes noncompartimentale et compartimentale de population. Les concentrations plasmatiques du *trans*-resvératrol en fonction du temps ont été décrites par un modèle

à un compartiment avec deux pics d'absorption. La pharmacocinétique du *trans*-resvératrol suite à une application topique est caractérisée par une clairance élevée et une cinétique de type 'flip-flop'.

Cette étude préclinique s'inscrit dans le cadre du développement d'un traitement éventuel pour les infections au HSV chez l'humain. À partir des données obtenues chez 3 espèces animales (souris, rat et lapin), les concentrations chez l'humain ont été prédites par allométrie. Cette méthode a prédit une dose topique efficace contre l'infection de l'herpès simplex chez l'humain de 292 mg de *trans*-resvératrol. Ainsi, suivant des doses topiques multiples de 300 mg, on obtient des concentrations simulées chez l'humain pouvant aller jusqu'à 25 µg/L. Ces concentrations faibles obtenues par simulation pourraient soutenir l'hypothèse courante dans la littérature selon laquelle certains conjugués du *trans*-resvératrol possèdent également une activité pharmacologique. Les résultats de l'analyse pharmacocinétique compartimentale et de l'allométrie présentés dans ce mémoire pourraient être utiles dans le processus de développement préclinique et clinique d'une formulation topique de *trans*-resvératrol.

Mots clés : *trans*-resvératrol, topique, crème, pharmacocinétique, noncompartimentale, compartimentale, population, allométrie

SUMMARY

Resveratrol (3,4',5-trihydroxystilbene) is a phytoalexin synthesized in certain plants as a defense response to UV or fungal attack. It exists in both cis- and trans-resveratrol isomeric forms. In addition to its wide spectrum of potential therapeutic effects, the inhibition of Herpes Simplex Virus (HSV) replication by trans-resveratrol may provide an effective treatment against chronic herpes infections. The objectives of this thesis were to 1) characterize the pharmacokinetics of trans-reveratrol in rabbits after application of topical trans-resveratrol creams and 2) predict a topical dose in humans using allometric scaling methodology.

Plasma trans-resveratrol concentrations observed after topical application of both creams confirm that the compound was able to diffuse through the skin layers and reach the basal epidermis, where active HSV replication occurs, and beyond. Trans-resveratrol concentrations obtained from a total of 24 rabbits that received multiple doses of either 12.5% or 19.0% trans-resveratrol cream for 28 consecutive days were analyzed using noncompartmental methodology, individual compartmental analysis (Adapt II®) and a population analysis (IT2S®). Comparative bioavailability of each formulation was assessed and pharmacokinetic parameters were determined using noncompartmental and population pharmacokinetic models. Plasma trans-resveratrol concentrations were best described by a 1-compartment model with double systemic absorption peaks. trans-Resveratrol pharmacokinetics after topical application was characterized by a high clearance and "flip-flop" kinetics.

The long-term goal of this preclinical study is the eventual treatment of HSV infections in humans. Allometric scaling from data obtained in 3 animal species

(mouse, rat and rabbit) to human predicted that a 292 mg topical trans-resveratrol efficacious dose would be required against HSV infection in humans. Simulations of multiple topical 300 mg doses in humans would yield plasma concentrations up to 25 μg/L. These low predicted concentrations may support current hypotheses in the literature that suggest possible pharmacological activity of trans-resveratrol conjugates. Results of compartmental PK analysis and allometric scaling described in this thesis may provide useful insight to provide optimal preclinical and clinical drug development.

Keywords: trans-resveratrol, topical, cream, pharmacokinetic, noncompartmental, compartmental, population, allometry

TABLE OF CONTENTS

LIST OF TABLES

LIST OF FIGURES

ABBREVIATIONS AND SYMBOLS

Δt	Discretisation time interval calculated as $t_{i+1} - t_i$
α	Alpha; proportion of administered drug being absorbed in first absorption peak
a	Coefficient or intercept of the line (allometric scaling)
Abs	Absorption
AIC	Aikaike Information Criterion
AUC	Area under the curve
$AUC_{0-\infty}$	The area under the curve from 0 to infinity, calculated as AUC_{0-t} + Clast/kel
AUC_{0-2}	The area under the curve from 0 to 2 hours postdose as calculated by the linear trapezoidal rule
AUC_{0-t}	The area under the curve from 0 to the last measurable concentration postdose as calculated by the linear trapezoidal rule
AUMC	The area under the moments curve defined as: $\sum_{i=1}^{n} (t_i * C_i + t_{i+1} * C_{i+1})/2 \cdot \Delta t$ where t_i = sampling time, C_i = concentration and $\Delta t = t_{i+1} - t_i$
b	Exponent or slope of the line (allometric scaling)
b[0]	Intercept of a line equation
b[1]	Slope of a line equation
b.i.d.	Two administrations per day
BLQ	Below the limit of quantitation

Abbreviations and Symbols (cont'd)

BW	Body weight
[^{14}C]	Radiolabeled with carbon-14
C*	Free-drug concentration at the skin target site
C_i	The plasma concentration at the ith sampling time (t_i)
CL or CL/F	The apparent total clearance
CLd/F	The apparent clearance in the peripheral compartment
Clast	The last measurable concentration in the concentration versus time profile
cm^2	Centimeter^2 (area)
Cmax	Maximum plasma concentration
$Cmax_{pred}$	Maximum predicted plasma concentration
Cpt	Compartment
CV	Coefficient of variability
CYP	Cytochrome p450 protein; followed by a family number indicating amino acid similarities; a capital letter denoting subfamily, and a number identifying a particular form
df	Degrees of freedom
Δdf	Difference in degrees of freedom calculated as df_1-df_2
Delay	Time delay to second absorption peak
Delay1;14;28	Time delay to second absorption peak on Day 1, 14, 28
DNA	Deoxyribonucleic acid
ECV	Estimation criterion value; also known as the objective function

Abbreviations and Symbols (cont'd)

EHC	Enterohepatic cycling
F	Bioavailability factor
GTS	Global two stage
h	Hour
HSV	Herpes simplex virus
HSV1; 2	Herpes simplex virus type 1 or type 2
ITS	Iterated two stage
IT2S	Iterative two stage software from Collins & Forrest
i.g.	Intragastric
i.p.	Intraperitoneal
i.v.	Intravenous
ka	Absorption rate constant
kel	Elimination rate constant
L	Liter
Lag	Time lag in absorption
Lag1; 14; 28	Time lag in absorption on Day 1; 14; 28
LC/MS/MS	Liquid Chromatography/Mass Spectrometry/Mass Spectrometry
LLOD	Lower limit of detection
LLOQ	Lower limit of quantitation
ln	ln-transformed
μ	Mean observed concentrations
mcg/ μg	Microgram

Abbreviations and Symbols (cont'd)

MAP	Maximum *a posteriori*
ml	milliliter
ML	Maximum likelihood
μM	Micromolar
MRT	Mean residence time
N	Total sample number
n	Partial sample number
No.	Number
N_{obs}	Number of observations
NDA	New Drug Application (FDA)
NONMEM	Nonlinear mixed effect modeling software from Sheiner & Beal
ng	nanogram
Np	Number of parameters
O_{ELS}	Extended Least Squares
O_{OLS}	Ordinary Least Squares
O_{wLS}	Weighted Least Squares
$\hat{O}_{wLS}$	Predicted weighted Least Squares
p.o.	*Per os*; oral administration
PD	Pharmacodynamics
PK	Pharmacokinetics
R^2	Coefficient of determination
R^2_1	Coefficient of determination of non-extrapolated concentrations

Abbreviations and Symbols (cont'd)

R^2_2	Coefficient of determination of extrapolated concentrations
$Resid_1$	Residual variability of non-extrapolated concentrations
$Resid_2$	Residual variability of extrapolated concentrations
σ^2	Variance
δ_{int1}	Intercept of non-extrapolated data
δ_{int2}	Intercept of extrapolated data
δ_{slope1}	Slope of non-extrapolated data
δ_{slope2}	Slope of extrapolated data
SC	Schwartz Criterion
SD	Standard deviation
STS	Standard two stage
T½ or $T_{½kel}$	Elimination half-life
$T_{½ka}$	Absorption half-life
t_i	The ith sampling time
TK	Toxicokinetics
UV	Ultraviolet
Var	Variance
Vc/F	The apparent central volume of distribution
Vp/F	The apparent peripheral volume of distribution
WRSS	Weighted residual sum of squares
Y_i	Observed concentration
$\hat{Y}i$	Predicted concentration

ACKNOWLEDGMENTS

I would like to express my sincere gratitude to Dr. Murray P. Ducharme for accepting to be my supervisor and allowing me the possibility of increasing my knowledge of pharmacokinetics, a field that I enjoy. His vast pharmacokinetic knowledge and experience, as well as his continuous support and excellent mentoring have been invaluable and very much appreciated while working on this study.

I would like to thank Dr. Jacques Turgeon for accepting to be my co-supervisor and for his insightful suggestions, pertinent questions and comments, which have been a tremendous help in the realization of this project.

I would also like to thank Dr. Tristan Booth, Chief Scientific Officer at Royalmount Pharma, for allowing me to work on this interesting project. The time he has allocated throughout this project as well as his support, guidance and scientific knowledge are very much appreciated.

I would like to thank Dr. Marika Di Marco for the generous amount of time she allocated to coaching my seminar presentation. Much of its success is due to her excellent advice and coaching skills and I am very grateful.

I would very much like to thank Dr. Fahima Nekka and Dr. France Varin for agreeing to be on this committee and for reviewing this thesis. I would also like to thank Andrée Mathieu, Vice-décanat aux études supérieures et à la recherche, for her help and professionalism in helping me fulfill University requirements.

I would like to thank Dr. Jean-François Marier for his time allocated to this project, scientific enthusiasm, pharmacokinetic knowledge and honest advice; Jean Lavigne for his excellent mathematic and computer skills; and Dr. Caroline Fradette and Nicola Will for their time allocated to this project.

I am very grateful to MDS Pharma Services for their generous grant so that I may complete my studies.

I would also like to express my heartfelt thanks to my husband, Tom Riel, and to my parents for their unwavering encouragement in my academic pursuits.

CHAPTER 1: INTRODUCTION

Resveratrol

Resveratrol (3, 4', 5-trihydroxystilbene) is a phytoalexin synthesized in certain plants as a defense response to UV or fungal attack (Hammond-Kosack and Jones 1996; Adrian et al. 2000). It exists in cis- and trans- resveratrol isomeric forms, with or without a glucoside moiety, with the trans isomer exhibiting a higher level of activity than its antipode (Figure 1.1). Resveratrol has been isolated from foods such as peanuts, soy, grapes and wine as well as from Itadori plant roots (*Polygonum cuspidatum)* used for centuries in China and Japan as a traditional herbal remedy (Burns et al. 2002). Interest in resveratrol by the scientific community was sparked in 1992-93 when epidemiological studies demonstrated a decreased incidence of cardiovascular diseases in Southern France even though dietary habits typically included high amounts of saturated fat. This contradiction was coined the "French Paradox". The mild to moderate consumption of wine, specifically the polyphenolic compounds in red wine such as resveratrol, has been associated with protective cardiovascular health benefits. Studies have since demonstrated additional possible resveratrol antioxidant activities such as lipid oxidation prevention (Frankel et al. 1993), platelet aggregation inhibition (Pace-Asciak et al. 1995), and modulation of nitric oxide production (Hattori et al. 2002).

Figure 1.1: The Structure of trans-Resveratrol

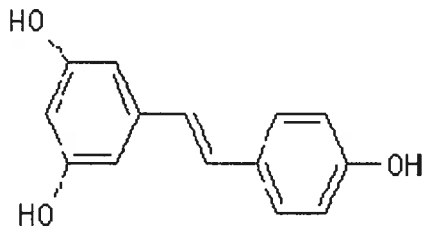

Initial publications of the potential beneficial cardioprotective effects of resveratrol have been followed by an expanding list of potential benefits published over the last decade. Briefly, these include extensive chemopreventive and anticarcinogenic activities (Jang et al. 1997; Ciolino et al. 1998; Huang et al. 1999; Park et al. 2001; Bhat and Pezzuto 2002), estrogenic properties (Gehm et al. 1997), anti-inflammatory effects (Donnelly et al. 2004), the activation of life-extending genes in yeast (Howitz et al. 2003) and the increased production of sperm in healthy rats (Juan et al. 2005). Anti-viral effects have also been demonstrated against HIV (Heredia et al. 2000) and the *herpesviridae* cytomegalovirus (Evers et al. 2004) and herpes simplex HSV-1 and HSV-2 (Docherty et al. 1999; 2004).

Resveratrol effect on Herpes Simplex Virus

The inhibition of herpes simplex virus (HSV) replication by trans-resveratrol may provide an effective treatment against chronic herpes infections. According to the Center for Disease Control, 70-90% of the general population carry HSV-1 and as many as one million are infected annually with HSV-2 in the United States (Fleming et al. 1997). Neonatal herpes infections may be extremely virulent and are associated with high mortality and morbidity. The most common transmission route is during delivery (Parker and Montrowl 2004). Controlling HSV infections, predominantly HSV-2, is highly desired due to its potential role as a co-factor in HIV transmission (WHO 2001).

During initial infection, the herpes simplex virus is transported by retrograde axonal transport to the nuclei of neurons near the local infection site (White and Fenner 1994). The virus then establishes a cycle of latent infection in neurons

followed by active replication occurring within 15 hours post infection in epithelial cells surrounding the oral, eye and genital areas (Docherty and Chopan 1974; Jenkins and Turner 1996). Thus, the virus has the ability to persist in its host indefinitely. No known cure exists; however, treatments are available for cutaneous outbreaks during active viral replication. Current treatments employ nucleoside analogues, from which acyclovir (Zovirax®) is the earliest, and most tested, treatment (De Clercq 2004). The mechanism of action involves acyclovir phosphorylation by viral *thymidine kinase*, followed by incorporation into replicating DNA by viral *DNA polymerase*. Acyclovir halts HSV replication through competitive inhibition and inactivation of *DNA polymerase* and by preventing further addition of nucleotides to the elongating DNA chain. Although acyclovir's advantage is its high specificity for HSV-infected cells due to its requirement of viral proteins for efficacy, its dependence on viral proteins also increases the probability of developing HSV resistant strains, which have indeed been isolated from immunocompromised patients, prompting more research into alternative forms of therapy (NDA 2002).

Trans-Resveratrol's inhibitory mechanism against HSV replication does not depend on activation by viral proteins, nor does it inactivate HSV directly or inhibit HSV entry into the cell *in vitro* (Docherty et al. 1999). Although the exact mechanism of action has yet to be elucidated, Docherty et al. have demonstrated resveratrol dose-dependent reversible inhibition of the cell cycle at the S-G2-M phase in healthy cells as well as the inhibition of immediate early viral protein production during the viral replication cycle *in vitro*. This inhibition by trans-resveratrol of regular cellular events and of early viral events may contribute to the disruption of the HSV replication cycle. *In vitro* trans-resveratrol concentrations of approximately

25-50 μg/mL appear to be efficacious against HSV replication. Interestingly, trans-resveratrol inhibits production of the essential immediate early regulatory viral protein ICP-4 required for HSV replication in epithelial (active phase) and neuron (latent phase) cells. Thus, resveratrol may have the ability to prevent reactivation of latent virus. This added potential therapeutic benefit is not possible with nucleoside analogue therapies because of their dependence on early viral enzymes produced only during the active phase of viral replication in epithelial cells.

Trans-Resveratrol efficacy *in vivo* was recently demonstrated on cutaneous HSV-1 infections in hairless mice (Docherty et al. 2004). Two creams containing 12.5% and 25% trans-resveratrol, as well as the 5% acyclovir ointment, were applied to the infected area of approximately 1-2 cm^2 on the dorsal aspect of the neck at various times after induced HSV cutaneous infection. Briefly, application of both trans-resveratrol formulations resulted in a significant decrease in HSV lesion formation compared to control, and with comparable efficacy to the 5% acyclovir ointment. The most effective results were obtained when trans-resveratrol cream was applied within 1-6 hours post infection, every 3 hours, 5 applications per day, for 5 days. There were no apparent indicators of dermal toxicity in the study animals at these doses.

Topical administration of trans-resveratrol

The results above demonstrate that an efficacious concentration of trans-resveratrol appeared to have reached the site of active HSV replication at the basal epidermis layer of the skin. After application of cream on the skin surface, trans-resveratrol must pass through the stratum corneum barrier and epidermis, presumably

by a series of complex, as yet unknown, processes prior to reaching the basal epidermis. Figure 1.2 illustrates the different layers in human skin.

Figure 1.2: The Structure of Human Skin

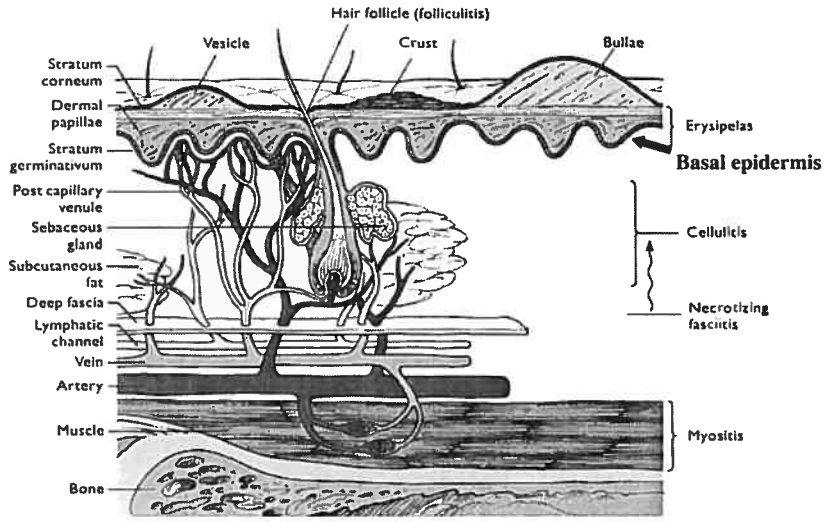

Source: http//www.images.MD/ Université de Montréal access

The skin is a multilayered membrane, which includes the stratum corneum, epidermis and dermis layers. Trans-resveratrol's diffusion across the stratum corneum could be a rate limiting process to reaching the basal epidermis. Studies using human skin have shown that the topical application of acyclovir ointment is less effective against HSV infection than oral or intravenous administration because of acyclovir's inability to efficiently penetrate the stratum corneum (Qureshi et al. 1998). The stratum corneum is an efficient barrier consisting of multiple lipid bilayers and anucleate keratinocytes whose main functions are to regulate water loss and halt entry of toxic materials (Williams 2003). Once cream is applied to the outer layer of the skin, passive diffusion through the stratum corneum potentially begins following water evaporation from the cream, which increases the concentration

gradient of trans-resveratrol solubilized in the formulation constituents, thereby driving permeation. Formulation enhancers, such as propylene glycol, reduce the skin barrier function altering diffusivity of the active ingredient through the skin (Smith et al. 1999). In addition, hydration of the stratum corneum will likely increase the drug permeation process dependent upon the polarity of the permeant (Flynn 1993). On the other hand, evaporation upon application of the cream changes the oil-water partitioning resulting in a surface residue. The degree of precipitation may completely halt the drug delivery process.

The passage of trans-resveratrol through the stratum corneum layer is followed by a partitioning step, then diffusion through the viable epidermis layer. The viable epidermis has a higher water content and is composed of living cells where contact may occur with metabolically active enzymes catalyzing phase I and phase II reactions (Hotchkiss 1998). Enzyme activity by cytochromes P-450 phase I enzymes such as CYP1A1, 1B1, 2B and 3A, and phase II enzymes such as UDP-glucuronosyltransferases and sulfotransferases has been observed in human skin, albeit at lower levels in comparison to their activity in the liver. Cutaneous loss of trans-resveratrol aglycone may be attributed to potential metabolism with these enzymes. For example, the biotransformation of trans-resveratrol to the active antileukemic agent piceatannol by CYP1B1 has been reported (Potter et al. 2002), as have conjugation reactions catalyzed by sulfotransferases (Yu et al. 2002) and various UDP-glucuronosyltransferases (Aumont et al. 2001).

Trans-Resveratrol is systemically absorbed via capillaries found in the dermis layer beneath the basal epidermis, the target area for topically applied trans-

resveratrol cream where active HSV infection occurs therefore, minimal systemic exposure would be preferred.

Pharmacokinetic Approaches

Pharmacokinetic analyses may provide some insight into the fate of trans-resveratrol following topical application. Pharmacokinetics is generally defined as the kinetic processes over time describing the absorption, distribution, metabolism and excretion of a drug administered to an organism (Shargel and Yu 1999). PK parameters are derived from observed drug concentrations, often obtained from blood and/or urine, plotted against their sampling times. Pharmacodynamics (PD) describes the desired physiological effect(s) of a drug at the site of action in the body, the 'biophase'. The biophase is often defined as the effect area surrounding the receptor, which initiates a cascade of desired events when bound to the drug (Bourne and von Zastrow 2004; Gabrielsson et al. 2000). If equilibrium is established between the drug concentration in the systemic circulation and at the biophase, therapeutic doses can be determined by measuring solely the drug concentration in the blood necessary to obtain the desired drug effect (PK/PD correlation).

The biophase where trans-resveratrol inhibition of HSV replication is likely to occur is in infected epithelial cells of the basal epidermis layer of the skin. Figure 1.3 is a simplified sketch of the potential movement of trans-resveratrol to the biophase after topical application.

Figure 1.3: trans-Resveratrol Biophase and Blood Compartments in the skin

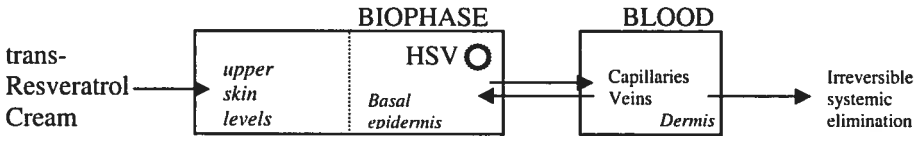

Figure 1.3 Possible routes of trans-resveratrol movement through the skin, biophase (site of action), and systemic circulation by absorption into the capillaries in the dermis layer of the skin. Theoretical trans-resveratrol re-distribution between the systemic circulation and the biophase is shown by the two-way movement between the blood and biophase "compartments".

Since only PK rather than PD analyses were performed for this research, the remaining introduction will focus on PK methodology. There are two main approaches used in PK analyses: 1) noncompartmental approach and 2) compartmental approach.

Noncompartmental Approach

The noncompartmental PK approach depends upon the following assumptions: 1) the drug follows linear first-order PK processes, 2) all drug molecules will be completely eliminated from the organism, and 3) the elimination process occurs from the sampling compartment (usually the circulatory system) (Gibaldi and Perrier 1982). This approach is based largely on the area under the curve (AUC) of the observed drug concentrations versus time (Figure 1.4).

Figure 1.4 Basic example of concentration versus time profile used in noncompartmental pharmacokinetics

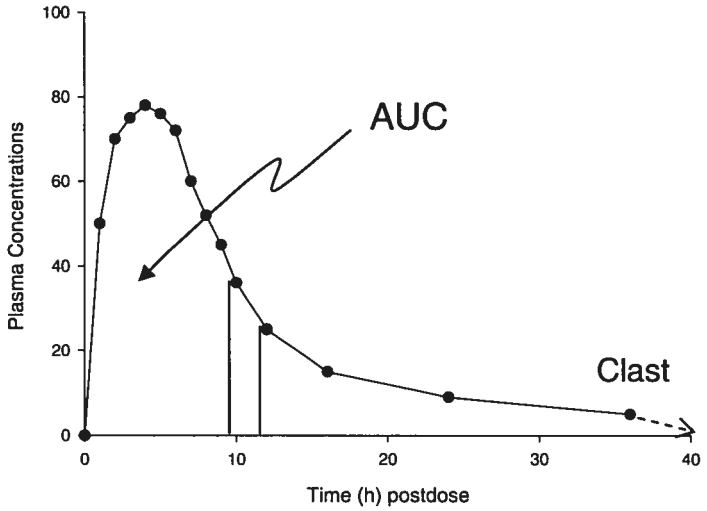

The AUC can be estimated using the linear trapezoidal rule (Gabrielsson and Weiner 2000) as follows:

$$AUC_{0-\infty} = \sum_{i=1}^{n} (C_i + C_{i+1})/2 \cdot \Delta t + C_{last}/kel$$

where C_i is the i^{th} concentration, C_{last} is the last measurable concentration, Δt is the discretisation time interval $t_{i+1} - t_i$ between concentrations and kel is the elimination rate constant. The AUC is dependent upon the number of blood samples where a richer sampling will result in a more accurate approximation of the true AUC. If the contribution at the last extrapolated trapezoid is significant (e.g. 20% or greater), the calculation of the AUC to infinity may not be considered robust. The AUC parameter over a specific dosing interval can determine whether there is evidence of drug accumulation following multiple doses under steady-state conditions. The $AUC_{0-\infty}$ calculated after a single dose should be equivalent to the $AUC_{0-\tau}$ at steady-state, where τ represents the dosing interval. This relationship is based on the

premise that the $AUC_{0-\infty}$ and $AUC_{0-\tau}$ characterize the extent of exposure of each drug molecule relative to the dose administered.

The AUC used in noncompartmental pharmacokinetics is derived by the theory of statistical moments (LeBlanc 1997). This theory introduces the area under the moments curve (AUMC) to describe the mean residence time (MRT) of a drug in the sampling compartment. The MRT is therefore only really obtainable after intravenous administration.

The following pharmacokinetic parameters may be determined using noncompartmental analyses (Gibaldi and Perrier 1982):

Parameter	**Description**
Cmax	Maximum observed plasma drug concentration in the concentration versus time profile.
AUC_{0-t}	The area under the curve from 0 to the last measurable concentration as determined by the linear or log-linear trapezoidal rule.
AUMC	The area under the moments curve defined as: $\sum_{i=1}^{n} (t_i * C_i + t_{i+1} * C_{i+1})/2 \cdot \Delta t$ where t_i = sampling time, C_i = concentration and $\Delta t = t_{i+1} - t_i$
MRT	AUMC/ AUC – Duration infusion/ 2
Kel	The elimination rate constant equivalent to the slope derived using linear regression of the ln(concentration) versus time.
T½	The elimination half-life defined by 0.693/kel.
CL/F	The total apparent drug clearance defined by: Dose/ $AUC_{0-\infty}$ (single dose) and Dose/ $AUC_{0-\tau}$ (steady-state), where τ is the dosing interval.

Compartmental Approach

The compartmental pharmacokinetic approach is based on the assumption that organisms are composed of a system of interconnected "well-stirred" compartments from which a finite number can be kinetically described in a model (Foster 2001). Often one assumes that each drug molecule has the same probability of transferring to or from a compartment, and that this transfer is governed by first-order conditions where the transfer rate of a drug molecule from one compartment to another is proportional to its concentration within the original compartment. An example is illustrated in figure 1.5.

Figure 1.5 Two-Compartment Pharmacokinetic Model

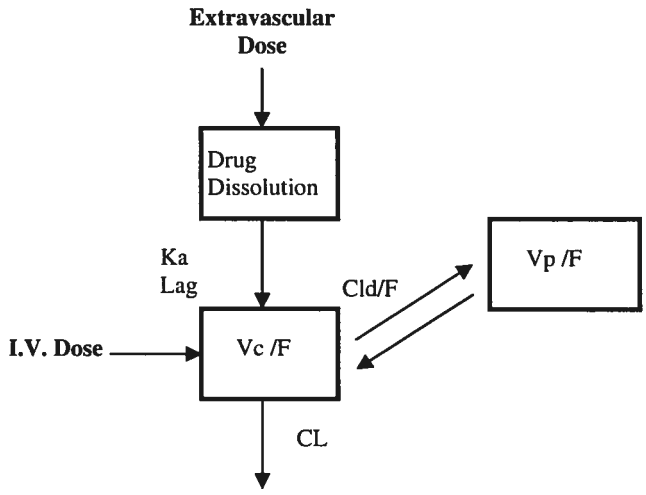

Linear PK models are described for a given range of doses by nonlinear regression models that generally take the following form: $Y = Ae^{-\alpha t} + Be^{-\beta t}$ where A, B, α, and β may be parameters estimated in a two-compartment model. After an extravascular dose such as p.o. administration, the drug dissolves in the gastro-intestinal "drug dissolution" compartment prior to being absorbed in the circulatory

system (Vc/F). The drug is immediately distributed into the circulatory system and periphery (Vp/F) and/ or is irreversibly eliminated (CL) from the organism. After an i.v. dose, the drug is immediately distributed into the circulatory system (Vc).

Parameter Estimation Procedure

The model-derived parameters attempt to describe the pharmacokinetic behavior of the observed concentrations (Y_i) while minimizing the difference between the observed and model-predicted concentrations ($\hat{Y}_i$).

Minimization Methods

Examples of minimization methods are presented below (Gabrielsson and Weiner, 2000):

(1) Ordinary Least Squares: $O_{OLS} = \sum_{i=1}^{n} (Y_i - \hat{Y}_i)^2$

(2) Weighted Least Squares: $O_{WLS} = \sum_{i=1}^{n} W_i(Y_i - \hat{Y}_i)^2$

(3) Extended Least Squares: $O_{ELS} = \sum_{i=1}^{n} [W_i(Y_i - \hat{Y}_i)^2 + \ln(\mathrm{var}(\hat{Y}_i))]$

(4) Generalized Least Squares = *step 1:* $O_{OLS;}$
step 2: O_{WLS} *where* $Wi = var(\hat{O}_{OLS})^{-2}{}_{step\ 1}$

where O is the objective function, Y_i is the observed concentration, $\hat{Y}_i$ is the model-predicted concentration and W_i is the applied weight. The applied weight may be the inverse variance attributed to the observation. Thus, observations that are more variable (less reliable) will theoretically contribute less to parameter estimation. The

generalized least squares method may be used to overcome limitations when the error variance is not normally distributed.

Algorithms designed to choose the most optimal parameter estimates using maximum likelihood (ML) are available for nonlinear models. ML is used to determine the most likely set of parameter estimates given the observed concentrations. One of the most robust algorithms is the Nelder-Mead simplex method (Gabrielsson and Weiner 2000). These complex computations require the plotting of the weighted residual sum of squares (WRSS) of each parameter to form a "simplex". The goal of this algorithm is to minimize this simplex by a defined criterion and select the optimal parameter solutions often called the "global minimum". Other less optimal solutions are referred to as "local minima".

Model Discrimination Criteria

Various statistical methods are used to select the best model from a pool of rival models. Specifically, these methods assess the goodness-of-fit of all models to a particular dataset and compare the statistical values. Examples of commonly employed methods are presented below: (Gabrielsson and Weiner 2000):

(1) ***F-test***

$$F\ statistic = \frac{/\underline{WRSS_1 - WRSS_2}/}{\underline{/df_1 - df_2/}} > F_{table}\,(0.05;\ \Delta df;\ df_2)$$
$$\frac{/\underline{WRSS_2}/}{df_2}$$

where df = degrees of freedom calculated as: Nobs - Np

The F-test is applied to compare hierarchical models, where one model can be deduced from the other (full versus reduced). The F distribution describes the probability that adding more parameters to a model will not change the WRSS. Therefore the difference $WRSS_1 - WRSS_2$ is theoretically zero. If the F statistic is greater than the F_{table} then the model with additional parameters is considered more appropriate.

(2) ***Akaike Information Criterion (AIC):***

$$AIC = N_{obs} \cdot ln(WRSS) + 2Np$$

where N_{obs} is the number of observations in the dataset, WRSS is the weighted residual sum of squares area or objective function, and Np is the number of parameters used in the model. The model with the lowest AIC real number value is generally deemed the most appropriate. The Np is added to the formula as a penalty factor. A model with more parameters than another must justify their inclusion by having a lower WRSS by a quantified amount. Thus, if two models have a different number of parameters but similar AIC values, the model with the lowest number of parameters will be judged the most appropriate model as dictated by the law of Parcimony.

(3) ***Schwartz Criterion (SC)***

$$SC = N_{obs} \cdot ln(WRSS) + Np \cdot ln(N_{obs})$$

This approach is based on the same principles as the AIC but with a stricter penalty proportional to the ln-transformed number of observations in the dataset.

(4)Residual Error or Variability Analysis

$$Resid = [\delta_{slope} + \delta_{int}/\mu] \times 100$$

where δ_{slope} represents the slope of predicted versus observed values, δ_{int} the intercept and μ the mean concentration values (observed or predicted). The residual variability is dependent on the variance model used and measures the amount of variability that cannot be explained by the model. Thus, residual variability is minimized.

(5) Estimation Criterion Value (ECV)

The ECV is the objective function as calculated in the minimization methods section above and is based on the WRSS, but without a penalty regarding the number of parameters used in the model. The ECV may therefore be smaller, and the AIC higher for models with a comparatively higher number of parameters for example, since the number of solutions available to the model is theoretically increased. Thus, a better fit may result in physiologically meaningless parameters. The ECV should be minimized with the caveat that the model with the lowest value may not be the most appropriate.

(6) Coefficient of Determination (R^2)

$$R^2 = 1 - \frac{\sum_{i=1}^{n} (Yi \cdot ti - \hat{Y}i \cdot ti)^2}{\sum_{i=1}^{n} (Yi \cdot ti)^2 - \sum_{i=1}^{n} (Y_i \cdot ti)^2} \cdot Wi$$

where $\hat{Y}i$ is the predicted value, *ti* is the corresponding sampling time and Y is the average of the observed values. A model that perfectly predicts the observed concentrations would yield a coefficient of determination equal to 1.

Population Pharmacokinetics

Population compartmental pharmacokinetic models attempt to describe the behavior of a drug in a target population with the aim of applying the model to individuals with similar characteristics (Jelliffe et al. 2002). Population PK parameters quantify 1) population mean kinetics, 2) inter-individual variability, and 3) intra-individual variability, assay error, and model error (Sheiner and Beal 1983). The population method is more advantageous than individual compartmental estimates because it more robustly assesses the residual error (point # 3). One can therefore attempt to explain the variability observed in patients with cofactors such as age and hepatic function, which may affect the PK behavior of a drug.

Two approaches to population modeling are: 1) Parametric and 2) Non-parametric.

Parametric

The parametric approach assumes the population parameters follow a known distribution, most commonly normal or log-normal (Jelliffe et al. 2000). One risk of assuming a normal distribution is not identifying subpopulations from which characteristics such as gender, age or smoking habits may affect the PK of a drug. PK parameters are estimated by measuring central tendency such as the mean or median. The two main approaches for estimating population parameters are the two-

stage methods, (for instance the standard two-stage (STS), iterated two-stage (ITS) and global two-stage (GTS) methods) and one-stage nonlinear mixed effect modeling (NONMEM) method.

Standard Two-Stage (STS)

This two-stage method first fits the individual data, and then population estimates are derived in a second step. The STS method derives the population estimates by providing descriptive statistics of PK parameters (i.e. average, standard deviations and correlation coefficients) of each parameter.

Iterated Two-Stage (ITS)

The ITS method begins by following the steps outlined for the STS method, then continues the analysis by comparing the parameter estimates to each patients' maximum *a posteriori* probability (MAP) (Jelliffe et al. 2002). Following this initial cycle, the parameter estimates may be used as priors to estimate new parameters and calculate new population means. This cycle continues iteratively until parameter convergence is obtained. The parameters and correlation coefficients are used at various intervals of the iterative process to measure the variance parameters *a posteriori.* The IT2S® software uses this method.

Nonlinear Mixed Effects Modeling (NONMEM)

Developed by Sheiner and Beal (Sheiner and Beal 1980), NONMEM is a widely used software that is very useful in, but not limited to, clinical environments where very sparse nonhomogeneous data collection often occurs. It is defined as a

one-stage approach because individual parameter estimates are not required and the dataset is analyzed globally. Individual PK parameters can also be provided in a post hoc analysis. The global goodness-of-fit is assessed by the objective function value based on the estimated parameters fitted by the extended least-squares minimization method. A decrease in the objective function value determines a better global fit. Advantages to using NONMEM include the addition of covariates such as creatinine clearance to explain inter-individual variability between patients, the use of a nonhomogeneous dataset obtained from patients in different clinical settings and model determination based on very sparse data from a specific patient population with applications for therapeutic drug monitoring.

Non-Parametric

The non-parametric approach does not make any assumptions regarding population parameter distributions. All model parameters are estimated for each subject and the probability of obtaining those parameters based on the observations is also estimated for each subject. Thus, this approach may be useful to identify any subpopulations that may be missed using parametric methods. Two widely used methods are the Nonparametric Maximum Likelihood (NPML) and Nonparametric Expectation Maximizing (NPEM) methods.

A comparison of the advantages and disadvantages of the different pharmacokinetic modeling strategies is tabulated below.

Table 1.1 Comparisons of Noncompartmental and Compartmental PK Approaches

	Noncompartmental PK	**Compartmental Individual PK**	**Compartmental Population PK**
Advantages	- Rapid - Simple - Robust - Independent of the analyst; model determination steps not required	- Drug may follow linear or non-linear PK - Accommodates all routes of drug administration - Moderately sparse sampling conditions - May provide insight into the PK activity of the drug - Mechanistic model linking PK and PD possible - Model simulations	- Drug may follow linear or non-linear PK - Accommodates all routes of drug administration - Sparse, very sparse nonhomogeneous sampling conditions - Intra-individual variability estimated; residual variability estimation more robust - May identify covariates contributing to parameter variability - Mechanistic model linking PK and PD possible - Dose determination in patients; therapeutic drug monitoring
Disadvantages	- Certain parameters can only be determined for IV drug administration - Requires rich sampling - One compartment approach - PK parameters dependent on the sampling schedule	- Time consuming: model determination process and analyses - Complicated - PK parameters not robust; high variability - intra-individual variability not computed	- Time consuming: model determination process and analyses - Complicated

Pharmacokinetic Modeling

Pharmacokinetic models are important because they reduce the mechanical complexity of drug kinetics in organisms to a more simplified form. This selective representation of reality has concrete applications such as predicting therapeutic dose ranges for a patient or estimating parameters not measurable *in vivo*, such as the absorption rate constant (Boxenbaum 1992). The decision to use noncompartmental versus compartmental modeling depends upon the specific type of knowledge desired from the data and the appropriateness of the method to obtain that knowledge (Foster 2001). Thus, noncompartmental and compartmental PK approaches can complement each other in acquiring pharmacokinetic information about a drug. As outlined in Table 1.1, the advantages and disadvantages of each method may dictate the best approach for answering specific questions about the data.

Trans-Resveratrol Pharmacokinetics

There are no known topical trans-resveratrol pharmacokinetic studies published in the literature. However, the PK behavior of oral and i.v. trans-resveratrol administered to laboratory animals and humans has been studied over the last decade and a brief overview of some of those results is presented. Trans-Resveratrol appears to be well absorbed after oral administration and highly metabolized to glucuronide and sulfonide conjugated forms, with resveratrol-3-sulfate being the primary conjugation metabolite in humans (Yu et al. 2003). Trans-Resveratrol was identified as a moderate inhibitor of CYP 3A4 and weak inhibitor of CYP 2C19. However, the sulfate metabolite was not an inhibitor of any of the CYP

enzymes used in the study. Oral (25 mg) and i.v. (0.2 mg) administration of [^{14}C]resveratrol to humans revealed three potential metabolic pathways including extremely rapid sulfate conjugation, glucuronic acid conjugation and hydrogenation, the latter, according to the authors, possibly produced by intestinal microflora (Walle et al. 2004). In addition, trans-resveratrol accumulation was observed in epithelial cells of the aerodigestive tract. Urine excretion appeared to be predominant, accounting for 53-85% of the oral dose and 42 – 83% after intravenous dose; recovery in feces reached 38% and 23%, respectively, and also contained the major resveratrol sulfate conjugate. Secondary peaks in the trans-resveratrol concentration profiles were attributed by the authors to enterohepatic cycling (EHC). Convincing evidence of its occurrence in rats has been demonstrated in a linked-rat model (Marier et al. 2002). The absorption of trans-resveratrol in the Walle study was high, about 70%, while the bioavailability was negligible which correlated with other published *in vivo* preclinical results (Andlauer et al. 2000; Kuhnle et al. 2000; Meng et al. 2004). In one study, the absolute bioavailability of trans-resveratrol in rabbits was approximately 1.5% and the elimination half-life was estimated to be 15 minutes following i.v. administration (Asensi et al. 2002). Preferential accumulation of radiolabeled trans-resveratrol and conjugates in mice occurred in the stomach, liver, kidney and intestinal tissues, as well as in the bile and urine (Vitrac et al. 2003).

Low trans-resveratrol bioavailability reported in many species, including humans, has resulted in speculation about the availability, and therefore possible desired biological activity, of non-metabolized trans-resveratrol. Efficacy has been reported at doses which would normally produce plasma levels below the 10 – 100 μM range apparently required for *in vitro* activity (Gescher and Steward 2003).

There appears to be a general consensus in the literature regarding this discrepancy between *in vitro* activity and *in vivo* bioavailability and the need to determine whether trans-resveratrol's *in vivo* pharmacological activity can also be attributed to its conjugates.

Allometry

Although the primary purpose of preclinical studies is to characterize the safety of a potential drug, preclinical studies are increasingly used to predict a drug's efficacious dose and pharmacokinetic behavior prior to dosing in humans. Allometry is one method used for this purpose.

Allometry is based on the fact that mammals of different sizes live for approximately the same amount of biological time. Since mammals breathe once every four heartbeats, approximately 200 million breaths and 800 million heartbeats are expected in a typical lifetime (Gould 1979). The relationship is characterized as follows:

$$\frac{\text{Breath time} = 0.0000470 \cdot BW^{0.28}}{\text{Heartbeat time} = 0.0000119 \cdot BW^{0.28}} = 4.02$$

where BW is the body weight. Many biological characteristics such as blood flow rate, size of capillaries, lung volume, etc., are functions of body weight (Calabrese 1984). Parameters that are a function of body weight and that also affect the PK of a drug may be predicted by allometric relationships across species. This premise is the basis for scaling preclinical pharmacokinetic parameters to humans.

The allometric method uses a power function $Y = aW^b$, which becomes a linear equation when plotted on a logarithmic scale: $\log(Y) = \log(a) + b \cdot \log(W)$ where

Y = parameter of interest

W = Body weight

a = coefficient or intercept of the line

b = exponent or slope of the line

Figure 1.6 is a generic example of an allometric scaling across species for a particular parameter. The allometric relationship is defined by the equation of the straight line derived by linear regression analysis. The regression line is generally extrapolated to a 70 kg weight for humans.

Figure 1.6: Graphic Representation of Allometric Scaling

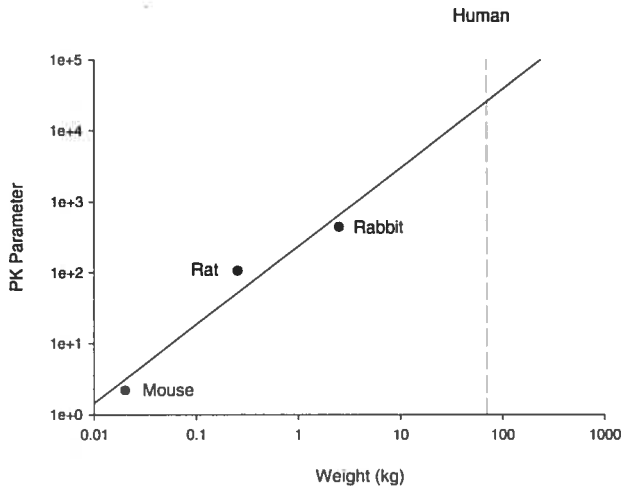

Objectives

There are two main objectives of the research described in this thesis:

1) Characterize the pharmacokinetics of two trans-resveratrol topical formulations after multiple topical applications to rabbits. Specifically, the bioavailability of each formulation is assessed and pharmacokinetic parameters are determined using noncompartmental and population pharmacokinetic models.
2) The long-term goal of these preclinical studies is the eventual treatment of HSV infections in humans. Therefore, an efficacious topical dose in humans is estimated via allometric scaling analyses using preclinical data in rabbits, as well as data from the literature.

CHAPTER 2: METHODOLOGY

Preclinical Study Design

Thirty New Zealand White Rabbits (15 males and 15 females) were divided into 4 primary groups, with one phase of the fourth group for toxicokinetic (TK) evaluation. The dose of trans-resveratrol cream applied for each treatment in each group is described in Table 2.1.

Table 2.1 - Quantity of trans-resveratrol cream applied per group:

Group	Quantity of Cream Applied (mg)	Formulation trans-Resveratrol (%)	trans-Resveratrol Dose Applied (mg)	Number of Animals	
				Primary	TK
1*	66	0	0	6	-
2	4	12.5	0.5	6	-
3	20	12.5	2.5	6	-
4	66	19.0	12.5	6	6

* Group 1 – Control group not included in the pharmacokinetic analyses.

An appropriate area on the upper dorsum was clipped free of hair close to the skin the day before the start of treatment and was carefully re-clipped or shaved with an electric razor as deemed appropriate throughout the study. A non-occluded dose of cream containing either 0%, 12.5% or 19.0% trans-resveratrol was applied using a gloved finger to a 4 cm^2 area approximately every 2 hours, 5 times per day, for 28 consecutive days. Gloves were changed between each group of animals. The number of treatments applied per day was based on previous efficacy studies of topical trans-resveratrol cream against HSV in a mouse model (Docherty et al. 2004). In addition, multiple applications per day followed by a long period without a dose (while asleep) mimic a standard topical treatment for HSV infections in humans. There were no apparent signs of toxicity or adverse dermal reactions at the dose levels tested in this study.

On Study Day 10, a change in washing procedure between doses was initiated. It appeared that the residue left over from a previous dose was not adequately removed after wiping the area with water. Therefore, a mild soap was also used for the remainder of the study. The addition of soap to the washing solution could have facilitated trans-resveratrol's diffusion across the skin layers by extracting lipids from the stratum corneum, which is known to decrease its barrier properties (Pugh 1999). Thus, there is a possibility that a lower amount of trans-resveratrol was absorbed into the systemic circulation after the first dose on Day 1 through to Day 9 compared to the amount absorbed after Day 10. However, a relative bioavailability factor did not improve the overall quality of fit in the population pharmacokinetic analyses (results not shown).

Blood samples were obtained from the central ear artery at the nominal times outlined in Table 2.2 below:

Table 2.2 – Pharmacokinetic Sampling Schedule

Groups	Formulation (% trans-resveratrol)	Dose (mg)	Sampling Schedule (h)		
			Primary Phase Days 1 & 28	TK Phase Days 1 & 28	Day 14
			0, 0.5, 2	0, 0.25, 0.5, 0.75, 1, 1.5, 2	0, 0.5, 2
2	12.5	0.5	√		
3	12.5	2.5	√		
4	19.0	12.5	√	√	√

Blood samples for groups in the primary phase were obtained on Days 1 and 28 before the first application of cream (0-hr) and at 0.5 and 2 hours thereafter. Blood samples were obtained for Group 4, TK phase at predose (0-hr) and at 0.25, 0.5, 0.75, 1, 1.5 and 2 hours postdose on Days 1 and 28, as well as at predose (0-hr) and at 0.5 and 2 hours postdose on Day 14.

Table 2.3 presents labels used throughout this thesis to reference the specific dose groups and formulations.

Table 2.3 – Animal dose group and formulation labels

Phase	Group No.	trans-Resveratrol Dose (mg).	Dose Group	Formulation (% trans-Resveratrol)	Corresponding Formulation No.
Primary (n = 18)	2	0.5	Low	12.5	I
	3	2.5	Mid	12.5	I
	4	12.5	High	19.0	II
TK (n = 6)	4	12.5	TK	19.0	II

Extrapolated trans-resveratrol Concentrations

Plasma trans-resveratrol was measured using a validated LC/MS/MS method, developed at MDS Pharma services, with a lower limit of quantification (LLOQ) of 4 ng/mL, an upper limit of quantification (ULOQ) of 1000 ng/mL, and a lower limit of detection (LLOD) of 1 ng/mL.

An aliquot of rabbit plasma containing the anti-coagulant EDTA, trans-resveratrol and the internal standard naringenin was extracted using a protein precipitation extraction procedure. The extracted samples were analyzed by high performance liquid chromatography equipped with an MDS Sciex mass spectrometer. Quantitation was by peak area ratio. Precision (%CV) and accuracy (%Theoretical) calculations for the quality control samples were less than 10% and 11%, respectively, which met the 15% acceptance criteria. Similarly, precision and accuracy results for LLOQ validation samples were 12.7% and 0.5% (inter-batch) and 17.9% and 3.0% (intra-batch), respectively, which satisfied the 20% acceptance criteria.

This study was the first to be performed in rabbits, therefore, there was a possibility that the predicted trans-resveratrol concentrations would not be observed at the administered doses. Indeed, only 44% of the blood samples were initially available for pharmacokinetic analyses because the remaining 56% were reported as below the LLOQ (BLQ). Since lowering the LLOQ was not possible, the concentrations between the LLOQ of 4 ng/mL and the LLOD of 1 ng/mL were extrapolated. The quantity of available samples was therefore increased to 75% and these extrapolated concentrations were included in all of the pharmacokinetic

analyses, however because they are not associated with the same certainty as the concentrations above the LLOQ, they were fitted with a separate variance model.

The analytical instrument had a lower sensitivity for calculating concentration values between the LLOD and LLOQ; consequently, it was assumed that extrapolated concentrations were more variable. For compartmental pharmacokinetic analyses, the variability associated with extrapolated concentrations was calculated separately; however, the weighting method was identical for all concentrations.

Handling BLQ Values

BLQ values flanked by measurable concentrations in the concentration versus time profiles are commonly handled by three different approaches: 1) they can be discarded (set as missing), 2) set at ½LLOQ, or 3) set to zero. There does not appear to be a general consensus as to which approach is best, as long as the method chosen is justified and consistently applied within the PK methodology. According to simulations performed by Stuart L. Beal (Beal 2001), setting the BLQ values as missing is the least biased method when applying compartmental and population PK models to data. Since it is erroneous to fit a value of zero using compartmental methods the BLQ values were set to missing for the compartmental and population PK analyses presented in this thesis. In addition, when faced with a sparse sampling design, Beal suggests that using ½LLOQ could be a useful approach. Thus, for the noncompartmental PK analysis presented in this thesis, BLQ values (< 1 ng/mL) flanked by measurable concentrations were set to ½LLOD or 0.5 µg/L. The alternative approaches of setting BLQ values as missing may overestimate the extent of exposure (AUC) in a sparse sampling situation and setting BLQ values at zero will

incorporate a negative bias since values flagged as BLQ values are actually somewhere between zero and the LLOQ (i.e. could never be less than zero). The impact of setting the BLQ values to ½LLOD will be covered in more detail in Chapter 3, which presents the noncompartmental results.

Noncompartmental Pharmacokinetics

The noncompartmental PK analyses were performed using PhAST® (Phoenix 1999) validated software. The maximum observed concentration, Cmax, was obtained directly from the observed concentrations versus sampling times. The extent of exposure from 0 to 2 hours postdose, AUC_{0-2}, was calculated for all dose groups even though in most cases only 2 postdose concentrations were available. Parameters $AUC_{0-\infty}$, kel and t½ could not be determined due to the sparse sampling and lack of terminal elimination in the profiles.

AUC_{0-2} was calculated using the linear trapezoid method. For some profiles, a log-linear approach may have been applicable due to apparent mono-exponential decreases in concentration within certain intervals. However, assuming first-order elimination, the linear trapezoidal rule tends to underestimate areas of increasing concentrations, and overestimate areas of decreasing concentrations. The AUC calculation using the linear trapezoid method was therefore deemed adequate for comparative purposes for all profiles in the current study, and was consistently applied as follows (Gabrielsson and Weiner 2000):

$$AUC_{0-2} = \sum_{i=1}^{n} (C_i + C_{i+1})/2 \cdot \Delta t$$

where C_i denotes the i^{th} concentration and Δt denotes the time interval between the C_i and C_{i+1} concentrations. AUC_{0-2} represents the area under the curve from zero until the last measurable concentration at 2 hours postdose.

The Cmax and AUC parameters were compared for evidence of trans-resveratrol accumulation for single versus multiple doses, as well as for any apparent differences in bioavailability between the two formulations. Median values were presented due to the high variability (30-160 CV%) observed between the PK parameters. Since the median represented the center value(s) of the specified dataset arranged in sequential order, this method of data presentation was judged to be the least influenced by very low or high values.

Compartmental Pharmacokinetics

Compartmental PK was performed with Adapt II® and population PK with IT2S®. These methods were chosen because they provide flexibility in model design and because the concentrations were obtained under controlled clinical conditions at specified sampling times.

Parameter Estimation

Individual compartmental PK parameters were estimated with Adapt II® software (D'Argenio and Schumitzky 1998) using maximum likelihood (ML) estimation, which derives the maximum probability of obtaining observed concentrations given the estimated parameters in the model. Ideally, parameter estimation minimizes the difference between the observed and predicted

concentrations. The weighted least squares method was used as a minimization method:

$$O_{wls} = \sum_{i=1}^{n} W_i (Y_i - \hat{Y}_i)^2$$

where O_{wls} is the objective function, W_i is an applied weight, Y_i is the i^{th} observed concentration and $\hat{Y}_i$ is the corresponding predicted concentration. A weight inversely proportional to the variance was applied in order to account for the variability in the data:

$$W_i = 1/\sigma_i^2$$

where σ_i^2 represents the variance associated with the observed value Y_i. The observed concentrations associated with a higher variance were attributed a smaller influence in the parameter estimations.

The variances associated with the observed concentrations were calculated as follows:

$$\sigma_{1i}^2 = (\delta_{int1} + \delta_{slope1} * Y_{1i})^2 \quad \text{(non-extrapolated concentrations)}$$

$$\sigma_{2i}^2 = (\delta_{int2} + \delta_{slope2} * Y_{2i})^2 \quad \text{(extrapolated concentrations)}$$

where the intercept includes errors associated with the analytical limit of detection and the slope includes errors associated with the observed concentration Y_i. Finally, the residual variability which represents a percentage of the data that could not be explained by the PK model was calculated as follows:

$$Resid_1\ (\%) = [\delta_{slope1} + \delta_{int1} / \mu_1]*100$$

$$Resid_2\ (\%) = [\delta_{slope2} + \delta_{int2} / \mu_2]*100$$

where μ_1 and μ_2 represent the mean observed concentrations for the non-extrapolated and extrapolated concentrations, respectively.

Model Discrimination

Various compartmental PK models were tested to find the least complex model that best predicted the observed plasma concentrations. The criteria used to distinguish between competing models were the Akaike Information Criterion (AIC), the estimation criterion value (ECV), residual variability, coefficient of determination (R^2), and visual inspection of individual profiles.

Population Pharmacokinetics

Once the final structural model was determined via compartmental methods, population analyses were performed using the iterative two-stage method with IT2S® (Collins and Forrest 1995). The first stage defined the kinetic parameters via the O_{wls} minimization procedure (described above) for each animal. The second stage estimated the population kinetic parameters by computing the parameter mean at the end of each iteration. Population mean variance and covariance were estimated *a posteriori* at various stages of the iteration process.

The groups that received the 12.5% trans-resveratrol cream were analyzed separately from those that received the 19% trans-resveratrol cream, and population parameters were derived for each formulation. Lag and delay parameters fitting the

Day 14 concentration data were included in the models only for groups that received the 19% trans-resveratrol cream.

The parameters associated with a lag time were estimated during the preliminary iterative processes. Once robustly estimated, they were fixed for each animal, and the population analyses were restarted.

Population Parameters

Means (CV%) were computed for all parameters in the model. The apparent clearance (CL/F), absorption half-life ($T_{½ka}$) and elimination half-life ($T_{½kel}$) were calculated for each animal using fitted population parameters as follows:

CL/F: kel*Vc/F

$T_{½ka}$: 0.693/ka

$T_{½kel}$: 0.693/kel

Allometric Scaling

So far, a limited amount of data has been published that describes the PK of trans-resveratrol in animals. Therefore, mean trans-resveratrol concentrations obtained from the literature (Asensi et al. 2002) were fitted using a compartmental approach with Adapt II® and the derived parameters were used for allometric scaling. Single doses of 20 mg/kg trans-resveratrol solution was administered via intra-gastric gavage to mice (0.02 kg weight), rats (0.25 kg) and rabbits (2.25 kg) and mean concentrations were best described by a two-compartment PK model. Total apparent clearance and volume of distribution were plotted against animal body weights on logarithmic scales. A regression line was obtained and PK parameters were extrapolated to humans with an approximate body weight of 70 kg.

The slope of the line was assumed to be independent of the route of administration since the same relationship across species would be observed using different routes of administration. Thus, the population apparent clearance (CL/F) and volume of distribution (Vc/F) of trans-resveratrol derived after topical application to rabbits was plotted on the graph and a new regression line was derived. Again clearance and volume of distribution were extrapolated to humans (70 kg) and also to mice (0.02 kg).

To derive an efficacious hypothetical dose in humans against HSV infection, a target AUC was estimated using allometric data in combination with published efficacy results in mice (Docherty et al. 2004). A 12.5% trans-resveratrol topical cream was one of the formulations used in the mouse efficacy study. Although the exact dose was not measured, the cream was applied to an area of approximately 1 to

2 cm^2. In the rabbit study, 4 mg of 12.5% trans-resveratrol cream, equivalent to a dose of 0.5 mg, was applied to an area of 4 cm^2. This corresponds to an estimated 1 to 2 mg of trans-resveratrol cream, equivalent to 0.125 mg and 0.25 mg doses, if applied to an area of 1 to 2 cm^2. These doses and allometric clearance in mice were used to estimate a targeted AUC that would be representative of efficacy against HSV:

$$AUC = Dose/ CL/F$$

The AUC corresponds to the possible extent of exposure required to inhibit HSV infection. The topical dose in humans that corresponds to this AUC will be estimated using the allometric clearance for topical administration in humans:

$$Dose = CL/F \times AUC$$

CHAPTER 3: RESULTS

Noncompartmental Pharmacokinetics

Plasma concentrations were first analysed using noncompartmental pharmacokinetic methodology. This section presents exploratory data analyses, noncompartmental PK parameter estimations, a bioavailability assessment of the two formulations tested and an analysis of the treatment of BLQ values in the determination of the extent of exposure of trans-resveratrol.

Preliminary Observations

The initial step, prior to determining any pharmacokinetic parameters, was to inspect the data by plotting the concentrations against sampling times. Individual, mean and median linear profiles from the 12.5 mg TK dose group are presented in Figure 3.1 due to this group's comparatively richer sampling schedule:

Figure 3.1 – Individual, Mean and Median Plasma trans-Resveratrol Concentrations on Day 1 (Figure 3.1a), Day 14 (Figure 3.1b) and Day 28 (Figure 3.1c) After Multiple Topical Administrations of 12.5 mg of 19% trans-Resveratrol cream for 28 Days to 6 Rabbits

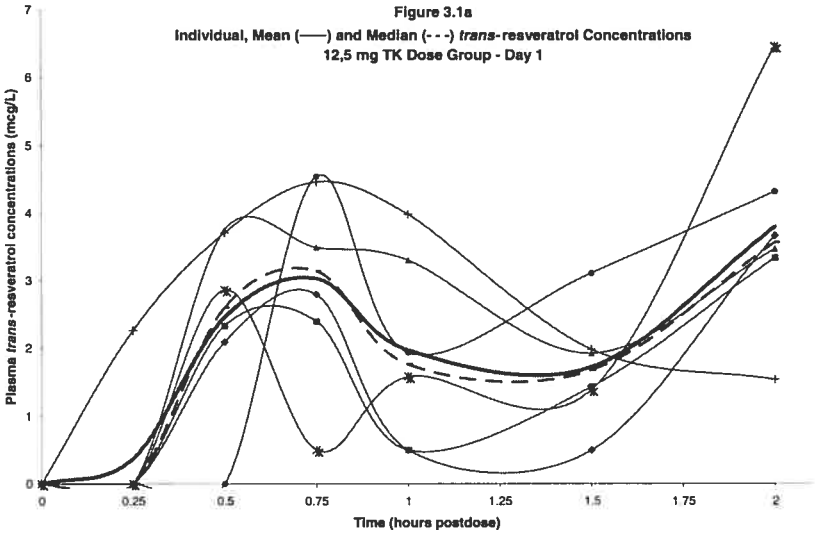

Visual inspection of the profiles on Day 1 showed at least two peaks in the systemic absorption of trans-resveratrol after a single topical dose. After an apparent lag time in the systemic absorption evidenced by the lack of measurable concentrations at 0.25 hours postdose, a first absorption peak occurred at approximately 0.5 to 0.75 hours post dose, followed by an apparent decrease in concentrations. At approximately 1.5 to 2 hours postdose concentrations increased again in what appeared to be the beginning of a second (or a third, as was the case for one rabbit) absorption peak. The mounting concentrations at the end of the profiles indicated that the drug had probably not been completely absorbed within the 2-hour dosing interval; thus, the rate of elimination could not be determined.

The individual profiles for the TK dose group on day 14 are shown in Figure 3.1b below.

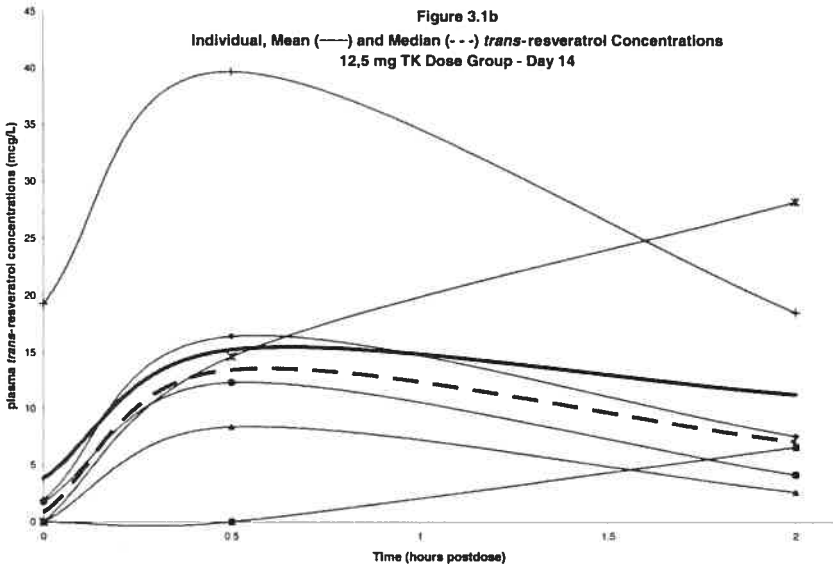

Mean (and median) plasma concentrations were approximately 5-fold greater on Day 14 than on Day 1. The 0.75-, 1- and 1.5-hour postdose samples obtained on Day 1 enabled the observation of multiple peaks in systemic absorption (Figure 1a). Multiple absorption peaks were not observed on Day 14, possibly due to the collection of only two postdose blood samples at 0.5 and 2 hours. The sparse sampling may have been insufficient to capture any multiple systemic absorption peaks similar to those observed in the profiles on Day 1.

The more extensive sampling schedule of Day 1 was repeated on Day 28 for the 12.5 mg TK dose group and the profiles are shown in Figure 3.1c below.

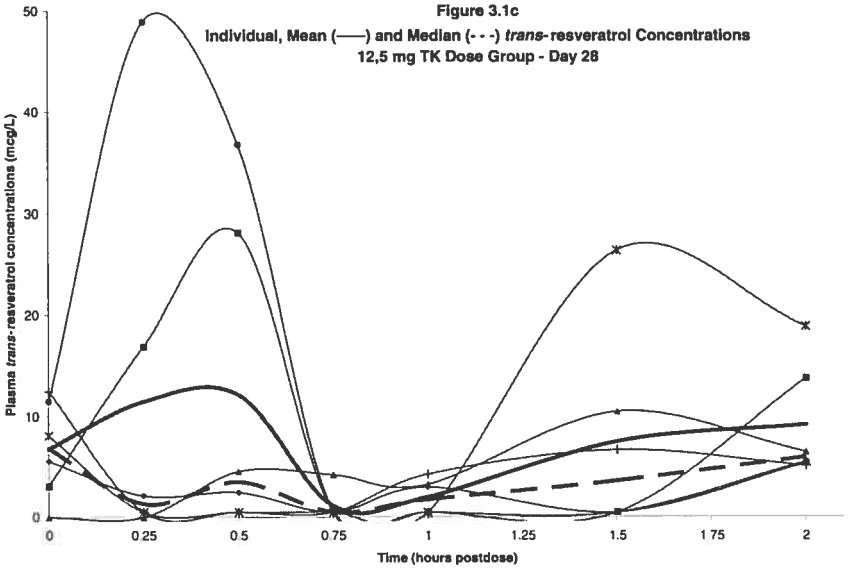

The profiles obtained for Day 28 also appeared to show multiple systemic absorption peaks and a lag time in absorption for some rabbits similar to the profiles on Day 1. In addition, higher concentration peaks were observed for some of the animals compared to the profiles on Day 1.

In summary, there appeared to be evidence of multiple absorption peaks within the two-hour sampling interval, with slight differences between the single and multiple dose profiles. However, the variability of the concentrations (CV% range 42 – 245) and sparse sampling conditions must be considered regarding any observed differences.

Pharmacokinetic Parameter Estimation

Prior to commencing the preclinical study, simulations were performed to predict Cmax values ($Cmax_{pred}$) for Day 1 after a single application of 0.5 mg, 2.5 mg and 12.5 mg trans-resveratrol cream. These simulations were based on results obtained after oral administration of trans-resveratrol in rats in a previous study

(Marier et al. 2002). A linear dose-concentration relationship and a similar relative bioavailability of the trans-resveratrol cream to that of orally administered trans-resveratrol were assumed. $Cmax_{pred}$ values, as well as the actual Cmax and AUC_{0-2} observed at the end of the study, are presented in Table 3.1 below.

Table 3.1 – Noncompartmental Pharmacokinetic Parameters (Range) of trans-Resveratrol in Plasma after Multiple Topical Applications of two formulations of trans-Resveratrol Cream for 28 Consecutive Days to Rabbits

Dose Groups	$Cmax_{pred}$* (µg/L)	Median (range) Pharmacokinetic Parameters				
		Cmax (µg/L)		AUC_{0-2}† (µg·h/L)		
		Day 1	Day 28	Day 1	Day 28	diff‡ (%)
12.5% Cream						
0.5 mg	6	4.63 (2–13)	4.85 (2-9)	3.58 (2-10)	5.13 (2-12)	43
2.5 mg	30	9.65 (2–14)	19.9 (2–86)	9.72 (2–16)	15.8 (1-115)	63
19.0% Cream						
12.5 mg	150	4.93 (3-18)	8.49 (2-49)	5.20 (3-23)	10.3 (3-25)	98

* Predicted Cmax concentrations for a single dose calculated prior to study start

† BLQ values flanked by measurable concentrations set to ½LLOD (0.5 µg/L)

‡ Percent increase in AUC_{0-2} from Day 1 to Day 28

The observed median maximum concentration (Cmax) of 4.63 µg/L in the 0.5 mg dose group on Day 1 was comparable to the predicted $Cmax_{pred}$ of 6 µg/L and the observed Cmax value of 4.85 µg/L on Day 28. The extent of exposure (AUC_{0-2}) after the first application on Study Day 1 (3.58 µg h/L) was comparable to the value observed on Day 28 (5.13 µg h/L), suggesting that there was minor accumulation of

trans-resveratrol after multiple applications of 0.5 mg of 12.5% trans-resveratrol cream.

For the 2.5 mg dose group the Cmaxpred value of 30 µg/L was not reached on Day 1 and the observed median Cmax increased from 9.65 µg/L to 19.9 µg/L after multiple applications from Day 1 through Day 28. A 63% increase in AUC_{0-2} was also observed, perhaps indicating that some accumulation may have occurred.

For the 19% trans-resveratrol cream formulation (12.5 mg dose), the observed median Cmax of 4.93 µg/L on Day 1 was significantly lower than the predicted value of 150 µg/L. This result was comparable to the median Cmax of 4.63 µg/L in the 0.5 mg dose group, which had a 25-fold lower dose. Two factors had not been considered when $Cmax_{pred}$ values were simulated: 1) the different properties of the two formulations, and 2) the quantity of cream applied for each dose level. These factors will be discussed in more detail in Chapter 4.

The median AUC_{0-2} values on Day 28 were approximately double the values observed on Day 1, suggesting some accumulation of trans-resveratrol following multiple applications of cream for 28 consecutive days. However, this trend was not conclusive due to the similar ranges observed for this parameter on Days 1 and 28 (3-23 and 3-25 µg·h/L, respectively).

Bioavailability Plots

The noncompartmental analysis appeared to demonstrate differences in the bioavailability of the two topical formulations. Although the 19% trans-resvertrol cream (12.5 mg) contained up to a 25-fold higher nominal dose than the 0.5 mg and 2.5 mg 12.5% formulation, a proportional dose-related increase in the rate and extent of exposure was not observed. Figures 3.2 and 3.3 represent a visual depiction of the relative differences in systemic bioavailability between these two formulations.

Figure 3.2 - Linear Plot of Cmax Normalized for Dose versus the Dose for the 0.5 mg and 2.5 mg groups (12.5% trans-resveratrol cream) and the 12.5 mg groups (19% trans-resveratrol cream)

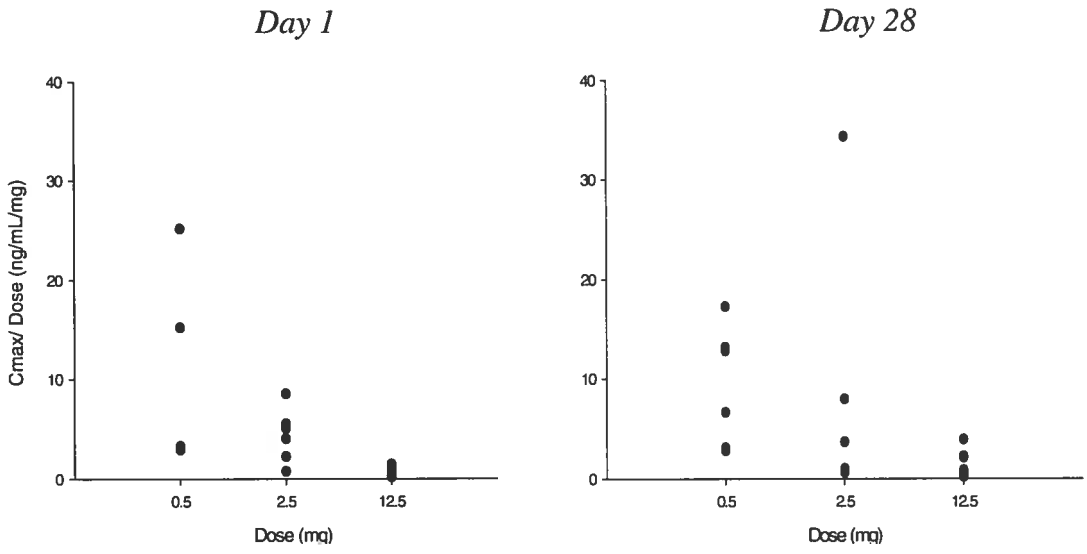

Figure 3.3 - Linear Plot of AUC_{0-2} Normalized for Dose versus the Dose for the 0.5 mg and 2.5 mg groups (12.5% trans-resveratrol cream) and the 12.5 mg groups (19% trans-resveratrol cream)

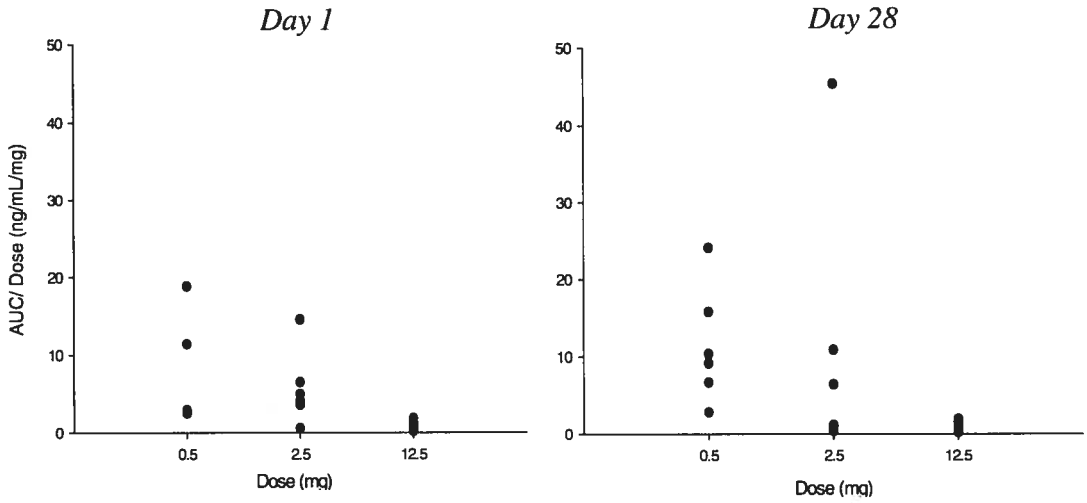

The 19% trans-resveratrol cream appears to be less bioavailable than the 12.5% formulation, as illustrated by the comparatively lower dose-normalized rate and extent of exposure on Days 1 and 28. It should be noted, however, that the amount of cream applied was significantly less for the 0.5 mg and 2.5 mg doses (4 and 20 mg per application, respectively) than the 12.5 mg doses (66 mg per application). This larger amount of cream applied, and not solely the percentage of trans-resveratrol contained within, may have contributed to the apparent lower bioavailability of the 19% trans-resveratrol cream. Factors that may have affected trans-resveratrol's bioavailability will be discussed in more detail in the Discussion section.

These noncompartmental pharmacokinetic results should be interpreted with caution due to the sparse sampling schedule and restricted analytical detection limit. Cmax and AUC_{0-2} may not have been adequately characterized for the groups in the

Primary Phase where profiles were described by only two postdose samples. The LLOD of 1 µg/L accounted for a large percentage of the median Cmax (5-22%) and AUC_{0-2} (6-28%) calculations. Consequently, the noncompartmental pharmacokinetic parameters presented above may not have been robustly assessed.

Treatment of BLQ Values

As discussed in Chapter 2, there are three generally accepted approaches to handling BLQ values flanked by quantifiable concentrations: 1) set the BLQ values as missing, 2) set them at ½LLOD or 3) set them at zero. The best approach in a noncompartmental model is the one that calculates the extent of exposure (AUC_{0-2}) with the least bias. This bias may be demonstrated best by comparing AUC_{0-2} calculations using all three approaches with data from the 12.5 mg TK dose group, which had the richest sampling schedule on Days 1 and 28. The data are shown in Table 3.2 below.

Table 3.2 – Noncompartmental Pharmacokinetic Parameter AUC_{0-2} Using Three Different Approaches for Handling BLQ Values in the 12.5 mg TK Group (19% trans-resveratrol)

BLQ Treatment	AUC_{0-2} (µg h/L) 12.5 mg TK group Median values	
	Day 1	Day 28
set to zero	4.06	12.7
set to ½LLOD (0.5 µg/L)	4.12	13.0
set as missing	4.69	25.6

Setting the BLQ values as missing for the 12.5 mg TK group significantly impacted the total extent of exposure on Day 28, accounting for approximately ½ the area when compared to the other two approaches (25.6 versus 13.0 µg·h/L).

Figure 3.4 compares the differences between AUC_{0-2} calculations in the profile of one rabbit from the 12.5 mg TK dose group when BLQ values are set to ½LLOD and to missing.

Figures 3.4a and 3.4b: Effect of BLQ Treatment on the Profile of Rabbit #20, 12.5mg TK Dose Group on Day 28

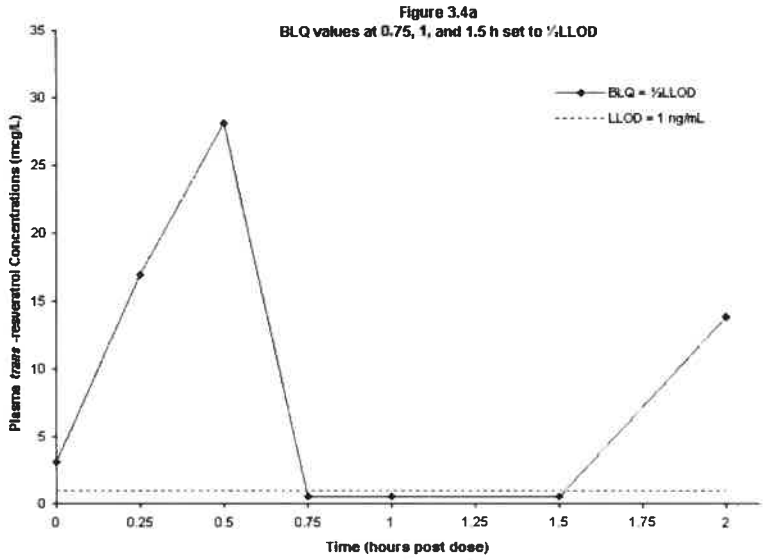

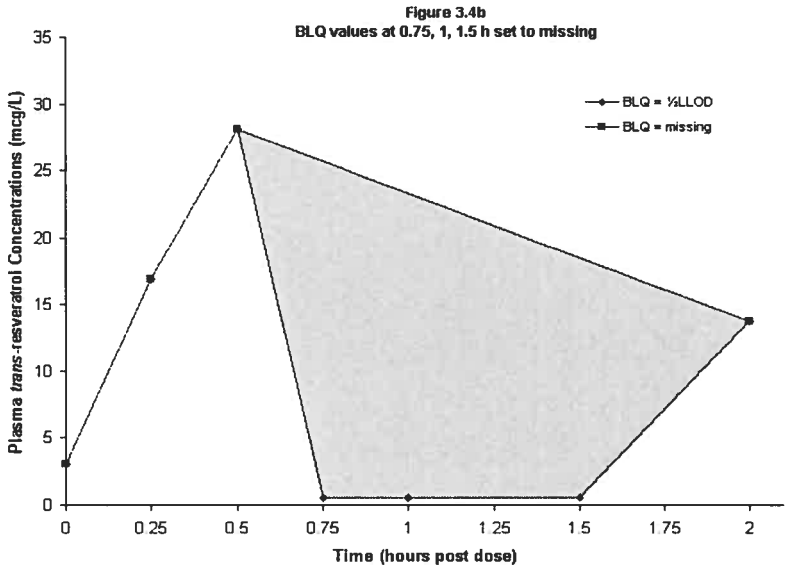

The shaded area represents the total extent of exposure (AUC_{0-2}) attributed solely to setting the BLQ values as missing at 0.75, 1 and 1.5 hours post dose. AUC_{0-2} was 15.6 µg·h/L when these BLQ values were set at ½LLOD and 39.5 µg·h/L when set as missing.

It should be noted that the sampling schedules did not include blood draws between 0.5 and 2 hours post dose (0.75, 1 and 1.5 hours) for three of the four dose groups. If all groups had multiple peaks and troughs similar to those observed in the 12.5 mg TK group, the AUC_{0-2} calculations for the three remaining groups may have been inflated.

The approach judged the least biased was to set BLQ values flanked by measurable concentrations to 1/2LLOD, or 0.5 μg/L. This approach appears to be the least biased due to 1) the sparse sampling, 2) the high frequency (47%) of BLQ values, and 3) the observed decreases in the extent of exposure, possibly due to multiple systemic absorption peaks as illustrated in Figure 3.1.

Compartmental Pharmacokinetics

Plasma concentration data were also analyzed using compartmental pharmacokinetic modeling. This section presents the results used to derive the final structural model prior to population PK analyses.

Model Determination

The compartmental pharmacokinetic models were written as first-order differential equations, and individual pharmacokinetic parameters were derived using maximum likelihood with Adapt II® software. The criteria used to discriminate between models were the minimum Aikaike information criterion (AIC), estimated criteria value (ECV), residual variability, maximum R^2 and visual inspection of the individual profiles. Various models were constructed and their capacity to fit the observed data was evaluated. These results are summarized in Table 3.3 below.

Table 3.3 - Derived (Median Value) and Calculated Parameters Used to Identify the Structural Compartmental Pharmacokinetic Model after Multiple Topical Applications of trans-Resveratrol Cream to Rabbits for 28 Days

Model	Description	AIC	ECV	$Resid_1$(%)	$Resid_2$(%)	R^2_1	R^2_2
Res1k	1 cpt basic	19.4	0.686	22.1	52.2	0.627	0.395
Res2k	2 cpt basic	20.6	-0.678	19.1	30.1	0.746	0.487
Res1a	1cpt, 1lag, 1 delay	12.2	-3.90	**17.3**	25.1	0.845	0.617
Res1d	**1cpt, 2 lags, 2 delays**	**10.7**	**-6.62**	18.4	**16.9**	0.903	**0.723**
Res3d	1cpt, 3abs, 2lags, 4 delays	22.8	-3.62	17.6	31.4	**0.907**	0.630

Note 1: Cpt = compartment, lag = time lag to initial systemic absorption, delay = time lag to second absorption peak, $Resid_1$ and $Resid_2$ = residual variability for non-extrapolated and extrapolated concentrations, respectively.
Note 2: Models Res1a and Res1d included 1 cpt, 2 absorption peaks and 1 ka in the model.
Note 3: Values in bold represent the best value for that particular parameter.

The pharmacokinetics of a topically administered trans-resveratrol cream to rabbits appears to be best described by the model Res1d which produced the lowest AIC and ECV values of 10.7 and -6.62, respectively. The amount of unexplained variability of 18.4% ($Resid_1$) and 16.9% ($Resid_2$) was relatively low while the R^2 values of 0.903 and 0.723 were comparatively high for the non-extrapolated and extrapolated concentration data, respectively. In addition, visual inspection of the individual profiles demonstrated good fits to the concentration data. Appendix 1 includes individual parameter estimates for this model as well as schematics of all rejected models included in Table 3.3. The final model is depicted in Figure 3.5 on the following page.

Figure 3.5- Final Model defined by one skin and central compartment and one rate of absorption defined by two absorption peaks and distinct lag and delay parameters for each of Day 1 and Day 28

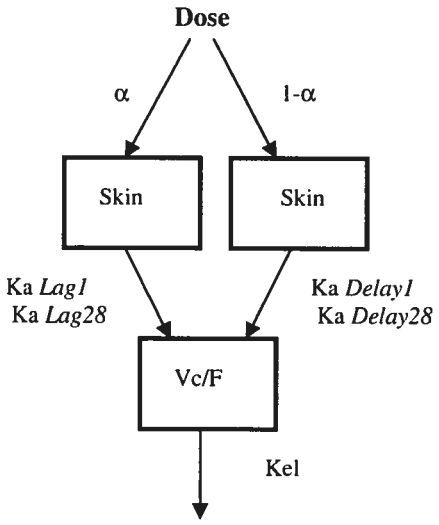

The final one-compartmental model (Res1d) includes skin and systemic blood compartments, one rate of absorption defined by two absorption peaks, as well as distinct lag and delay parameters for each of Day 1 and Day 28. "Dose" represents a single application of cream followed by proportional quantities (α and 1-α) of trans-resveratrol absorption through the layers of the skin. The compound is subsequently absorbed (ka) into the systemic circulation (defined by Vc/F) and a time delay in the absorption associated with the proportion (1-α) of trans-resveratrol defines a second absorption peak through the skin. The plasma concentrations predicted by the model are based on the volume of distribution (Vc/F) of the systemic circulation also estimated by the model. The drug undergoes elimination from the central compartment by a first-order rate constant of elimination.

The final model was described in a FORTRAN file using differential equations:

$$\frac{dX1}{dt} = R(1) \cdot \alpha - ka \cdot X1 \cdot Z$$

$$\frac{dX2}{dt} = R(1) \cdot (1-\alpha) - ka \cdot X2 \cdot Z1$$

$$\frac{dX3}{dt} = R(2) \cdot \alpha - ka \cdot X3 \cdot Z2$$

$$\frac{dX4}{dt} = R(2) \cdot (1-\alpha) - ka \cdot X4 \cdot Z3$$

$$\frac{dX5}{dt} = ka \cdot X1 \cdot Z + ka \cdot X2 \cdot Z1 + ka \cdot X3 \cdot Z2 + ka \cdot X4 \cdot Z3 - kel \cdot X5$$

where:
Z=0; IF (time > lag1) Z=1
Z1=0; IF (time > lag1+ delay1) Z1=1
Z2=0; IF (time > lag28) Z2=1
Z3=0; IF (time > lag28+ delay28) Z3=1

$$\hat{Y}_i = \frac{X5}{Vc_i/F}$$

R(1) represents the doses applied from Day 1 to Day 27 and R(2) represents the dose applied on Day 28. The amount of trans-resveratrol in each box is represented by X1 to X5 and the flag parameters Z to Z3 code the lag and delay parameters. All BLQ values were set as missing for compartmental PK analyses.

Population Pharmacokinetics

The sparse sampling conditions necessitated population PK analyses to robustly determine the pharmacokinetic parameters. Median values of the final model parameter estimates derived with Adapt II® were used as beginning priors for the population PK analysis, performed using an iterative two-stage methodology in IT2S®.

Population PK Parameter Estimates

The population parameters were evaluated separately for each formulation and parameter estimates obtained from IT2S® using the final model are presented in Table 3.4.

Table 3.4 – Estimated mean population parameters and their percent coefficient of variation for trans-resveratrol after multiple topical applications of 12.5% or 19.0% trans-resveratrol cream to rabbits for 28 consecutive days

		12.5% trans-resveratrol cream		19% trans-resveratrol cream	
Parameters		Mean	CV%	Mean	CV%
α	*(%)*	5.00	72.2	13.9	39.3
Ka	*(h^{-1})*	0.122	36.3	0.185	33.4
Vc/F	*(L)*	3.20	73.8	9.13	16.3
Kel	*(h^{-1})*	7.51	42.6	8.49	19.9
CL/F	*(L/h)*	21.5	86.7	75.3	8.4
$T_{½ka}$	*(h)*	7.06	81.4	4.26	41.9
$T_{½kel}$	*(min)*	7.76	60.6	5.11	23.6
Lag1	*(h)*	0.15	60	0.19	36.2
Delay1	*(h)*	0.38	138	1.80	4.12
Lag14	*(h)*	…	…	0.25	60.7
Delay14	*(h)*	…	…	1.42	44.4
Lag28	*(h)*	0.30	187	0.54	101
Delay28	*(h)*	0.94	86	1.92	32.3

Note: CL/F, $t_{½ka}$ and $t_{½kel}$ are calculated pharmacokinetic parameters

The two-absorption peak model produced good fits to the observed concentrations after multiple topical applications of trans-resveratrol cream to rabbits. Individual graphs for all animals are presented in Appendix II and Individual PK parameters are presented in Appendix III. The inter-individual variability (CV%) of the population parameters obtained using IT2S® (Appendix III) was lower than the variability of the individual parameters obtained using Adapt II® (Appendix II).

Goodness-of-fit (Figures 3.6 through 3.9) demonstrate a good correlation between predicted and observed concentrations as well as balanced weighted residuals versus observed concentrations.

Figure 3.6: 12.5% trans-Resveratrol Cream Population Predicted versus Observed Concentrations Using the Final Model in IT2S®

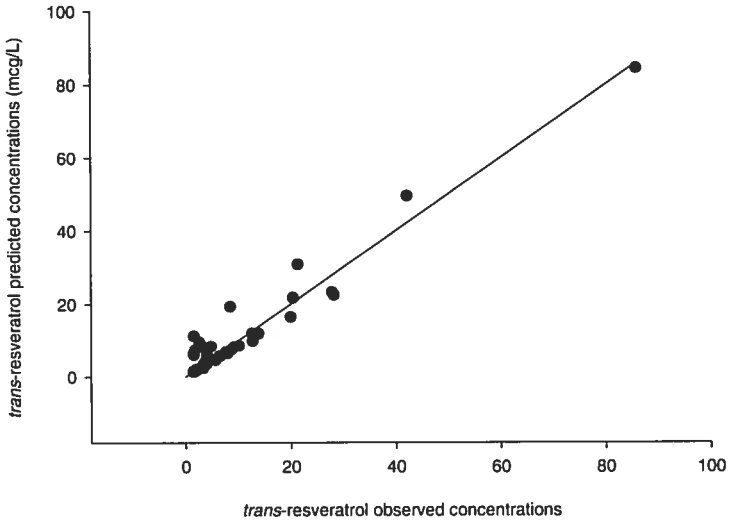

Figure 3.7: 19.0% trans-Resveratrol Cream Population Predicted versus Observed Concentrations Using the Final Model in IT2S®

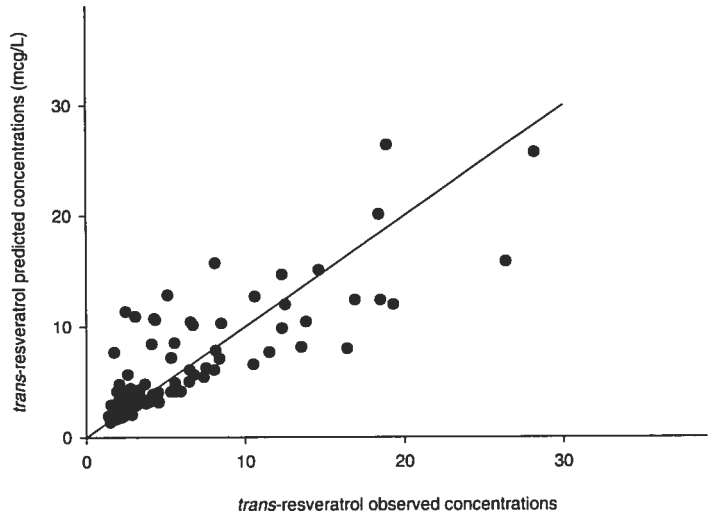

Figure 3.8: 12.5% trans-Resveratrol Cream Weighted Residuals versus Observed Concentrations Using the Final Model in IT2S®

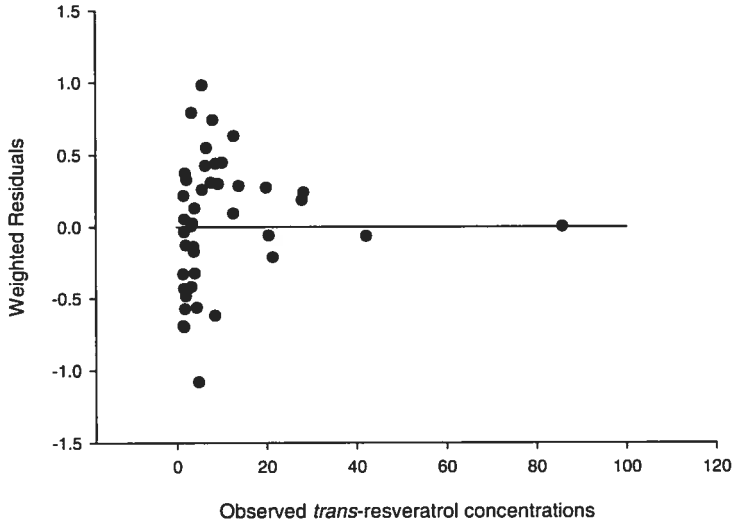

Figure 3.9: 19.0% trans-Resveratrol Cream Weighted Residuals versus Observed Concentrations Using the Final Model in IT2S®

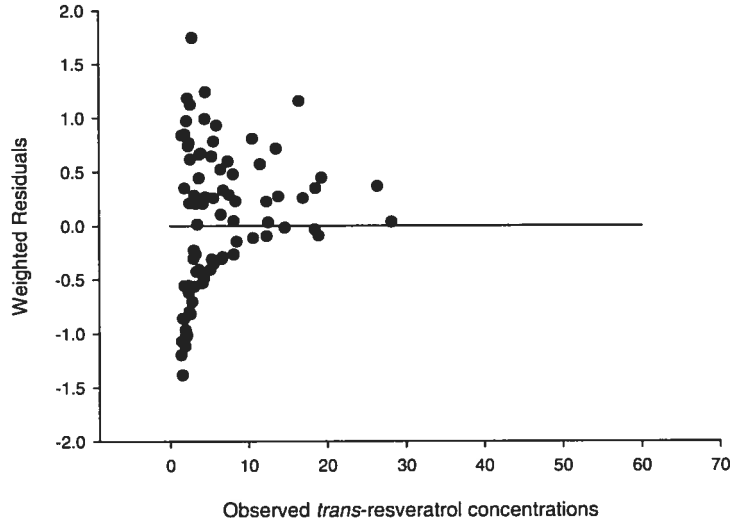

Allometric Scaling

As detailed in the previous chapter, mouse, rat and rabbit mean trans-resveratrol concentration data from the literature (Asensi et al. 2002) were fitted using a two-compartment model and PK parameters were estimated (the profiles and relevant pharmacokinetic parameters are included in Appendix IV) and used in the allometric results presented below. The allometric relationships for the peripheral volume of distribution (Vp/F) and clearance (Cld/F) fitted by the two-compartment model are also included in Appendix IV for information purposes.

Allometric PK Parameter Results

The estimated PK parameters versus animal body weights were plotted on logarithmic scales and a line equation [Yi = intercept + Xi(slope)] was derived for each parameter using linear regression analysis. The predicted apparent volume of distribution (Vc/F) and clearance (CL/F) in humans were extrapolated from these line equations as shown in Figures 3.10 and 3.11 below.

Figure 3.10a Allometric Prediction of Volume of Distribution (Vc/F) in Humans after Oral (•) Administration in the Mouse, Rat and Rabbit

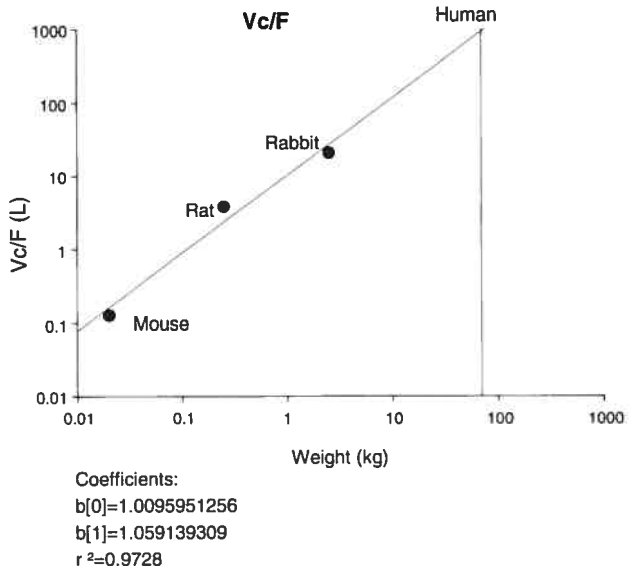

The total apparent volume of distribution was plotted against the respective animal body weights on logarithmic scale. A regression line was obtained and a volume of distribution was extrapolated to humans with an approximate body weight of 70 kg, as shown by the intersection between the regression and vertical lines on the graph.

Figure 3.10b Allometric Prediction of Volume of Distribution (Vc/F) in Humans after Oral (•) Administration in the Mouse, Rat and Rabbit, and Topical 12.5% trans-Resveratrol Cream (▲) and 19% trans-Resveratrol Cream (■) Administration to Rabbits

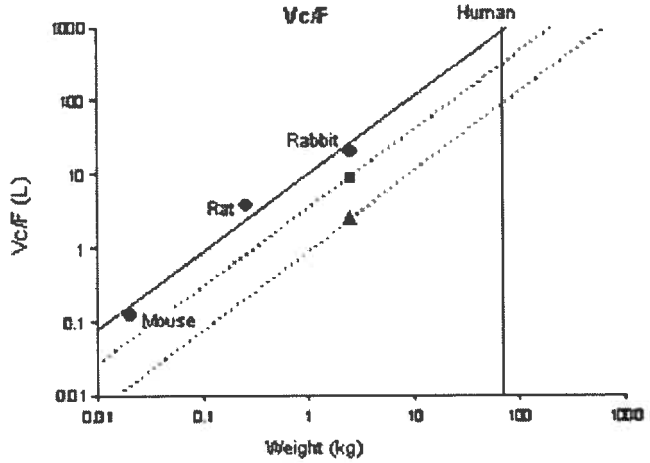

The line equations for the topical formulations were derived in two steps, and were based on the assumption that the slopes were identical, or the same relationship across species would be observed, for both oral and topical routes of administration. First, the intercepts were calculated for each topical formulation using the respective slopes (coefficient b[1]) from the oral data and the mean population parameters in rabbits (Table 3.4). Second, derived line equations were used to extrapolate the apparent volume of distribution of topically administered trans-resveratrol to humans.

Figure 3.10c : Allometric Prediction of Volume of Distribution (Vc/F) in Humans after Topical 12.5% trans-Resveratrol Cream (▲) and 19% trans-Resveratrol Cream (■) Administration to Rabbits

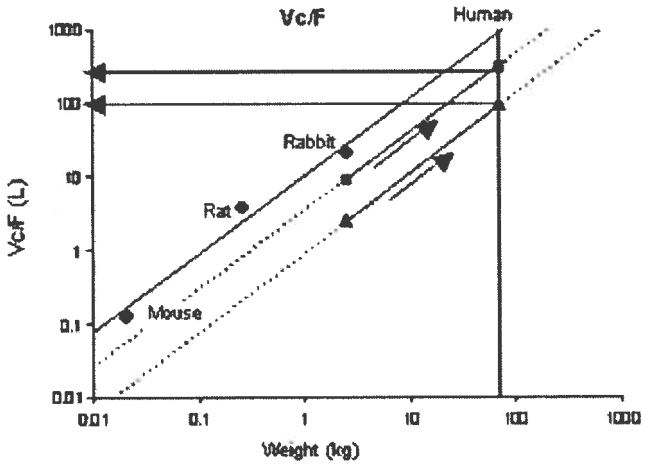

The arrows in the figure above indicate the extrapolated volume of distribution in humans predicted for topical application of both formulations of trans-resveratrol cream.

These steps were repeated in order to determine the total apparent clearance in humans as shown in Figure 3.11.

Figure 3.11a : Allometric Prediction of Clearance (CL/F) in Humans after Oral (•) Administration in the Mouse, Rat and Rabbit.

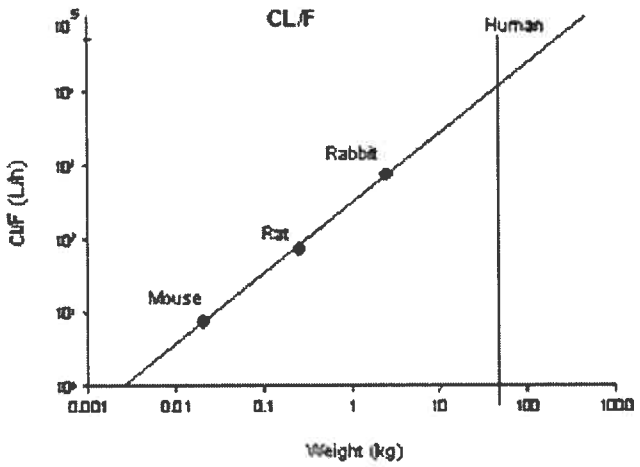

Coefficients:
b[0]=2.4762595462
b[1]=0.9511529895
r²=0.9981

Figure 3.11b : Allometric Prediction of Clearance (CL/F) in Humans after Oral (•) Administration in the Mouse, Rat and Rabbit, and Topical 12.5% trans-Resveratrol Cream (▲) and 19% trans-Resveratrol Cream (■) Administration to Rabbits

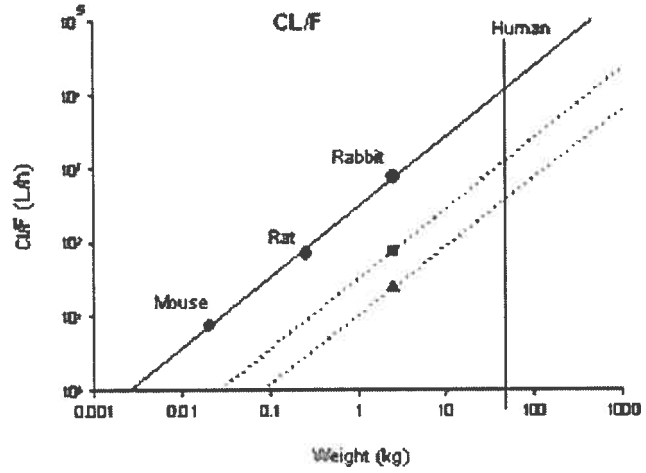

Figure 3.11c : Allometric Prediction of Clearance (CL/F) in Humans after Topical 12.5% trans-Resveratrol Cream (▲) and 19% trans-Resveratrol Cream (■) Administration to Rabbits

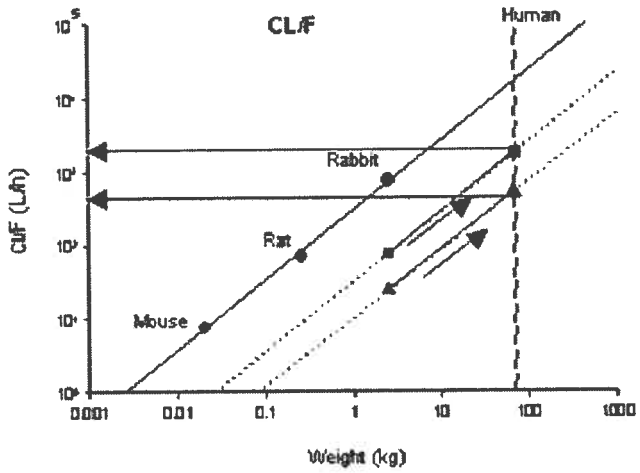

The arrows in the figures above indicate the extrapolated total apparent clearance in in humans.

In summary, the volume of distribution and total apparent clearance PK parameters predicted in humans after topical administration were calculated using the following line equations:

12.5% trans-Resveratrol Cream:

$$Vc/F = \text{antilog}\,[0.0836761 + (1.845098 \times 1.0591393)]$$

$$CL/F = \text{antilog}\,[0.9539366 + (1.845098 \times 0.95115299)]$$

19% trans-Resveratrol Cream:

$$Vc/F = \text{antilog}\,[0.538996872 + (1.845098 \times 1.059139309)]$$

$$CL/F = \text{antilog}\,[1.498293147 + (1.845098 \times 0.95115299)]$$

where human body weight = log(70kg) = 1.845098. Allometric scaling PK Parameter Results are presented in Table 3.5 below.

Table 3.5 Allometric Scaling PK Parameters

Species*	Oral†	Topical‡	
	intra-gastric (20 mg/kg)	12.5% Cream	19% Cream
	Volume of Distribution (Vc/F) (L)		
Mouse	0.128	0.0192	0.0549
Rat	3.86	…	…
Rabbit	20.8	3.20	9.13
Human	920	109	311
	Clearance (CL/F) (L/h)		
Mouse	7.66	0.218	0.763
Rat	71.3	…	…
Rabbit	760	21.5	75.3
Human	17031	511	1792

* Body Weights: Mouse = 0.02 kg, Rat = 0.25 kg, Rabbit = 2.5 kg, and Human = 70kg

† Fitted (mouse, rat and rabbit) and extrapolated (human) PK parameters (figures 3.10 and 3.11)

‡ Fitted PK parameters for rabbit (shown in Table 3.4); mouse and human parameters extrapolated (Figures 3.10 and 3.11)

Predicted Topical Dose in Humans

Previous results from the mouse efficacy study demonstrated that applying a 12.5% trans-resveratrol cream significantly inhibited HSV lesions (Docherty et al. 2004). Using the extrapolated apparent clearance of 0.218 L/h in mice for this formulation, an efficacious AUC could be estimated:

$$\begin{aligned} AUC &= Dose/\ CL/F \\ &= 0.125\ mg/\ 0.218\ L/h \\ &= 0.573\ mg{\cdot}h/L \end{aligned}$$

Assuming linear pharmacokinetics, it follows that a dose of 0.25 mg would double the effective AUC to 1.15 mg·h/L. In addition, the cream was applied every 3 hours in the mouse study, corresponding to possible average concentrations (Cave) of 0.191 mcg/L to 0.382 mcg/L in mice.

The efficacious AUC is the theoretical target for effective HSV inhibition in humans. The topical dose in humans can be estimated using the extrapolated CL/F in humans for the 12.5% trans-resveratrol formulation:

$$\begin{aligned} \text{Dose in Humans} &= AUC \times CL/F \\ &= 0.573\ mg{\cdot}h/L \times 511\ L/h \\ &= 292\ mg \end{aligned}$$

Simulations were performed using a 300 mg topical dose of 12.5% trans-resveratrol, an apparent clearance of 511 L/h and volume of distribution of 109 L in humans: Due to the long absorption rates of trans-resveratrol administered as a cream formulation some accumulation is expected.

Figures 3.12a – 3.12d: Simulations in Humans using the Final Model with Varying ka (h^{-1}) and alpha (%) after 300 mg trans-resveratrol topical doses of 12.5% trans-resveratrol cream, Every Two Hours for a Total of Five Applications

Figure 3.12a: ka = $0.2h^{-1}$; alpha = 10%

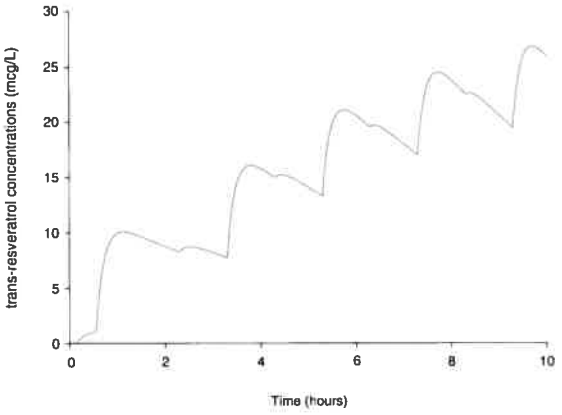

Figure 3.12b: ka = $0.1h^{-1}$; alpha = 5%

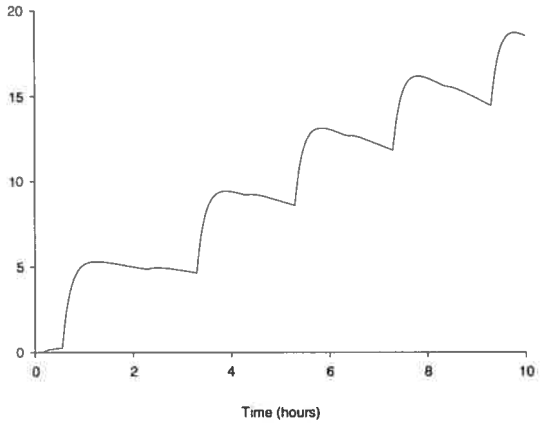

Figure 3.12c: ka = $0.05h^{-1}$; alpha = 10%

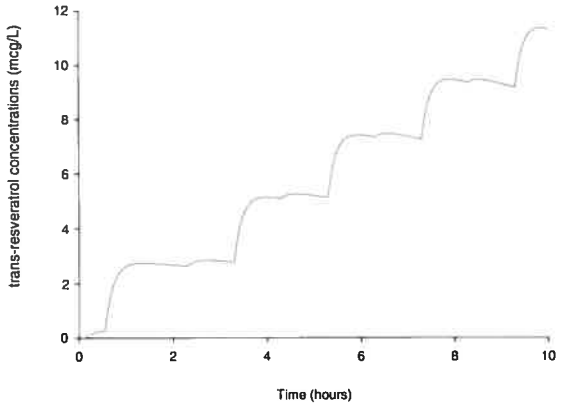

Figure 3.12d: ka = $0.1h^{-1}$; alpha = 25%

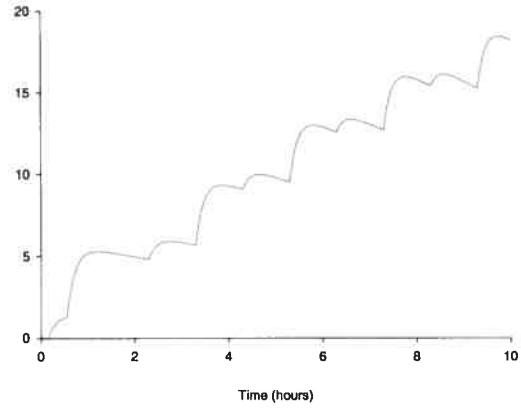

Four scenarios were simulated using the final model with varying combinations of trans-resveratrol absorption rates (ka) and the proportion of drug absorbed in the first absorption peak (alpha). The values chosen for these parameters

were based on the population PK results obtained for the 12.5% trans-resveratrol cream in rabbits (Table 3.4). The highest predicted plasma trans-resveratrol concentration of approximately 25 mcg/L in humans was observed after simulating 5 cream applications using an absorption rate (ka) of 0.2 h^{-1} (Figure 3.12a).

CHAPTER 4: DISCUSSION

Pharmacokinetic Modeling

A compartmental model was designed to describe the pharmacokinetics of trans-resveratrol after multiple topical applications of two cream formulations. Multiple peaks observed in some of the profiles were pivotal for designing the final model. Given the high variability of the plasma concentrations obtained from a sparse sampling schedule, the use of population PK methodology in IT2S® (Appendix III) gave more robust estimates of the model PK parameters than Adapt ® (Appendix I).

Multiple topical administrations of trans-resveratrol appeared to be well described by a two absorption peak model. Individual profiles showed increased plasma concentrations at the end of the profiles, possibly due to a second absorption peak. The PK of trans-resveratrol was characterized by a one compartmental model with linear elimination. Although glucuronidation and β-glucuronidase cleavage of trans-resveratrol is theoretically possible in rabbits (Dulik and Fenselau 1987; Davies and Morris 1993), enterohepatic circulation governed by bile release, cleavage and intestinal reabsorption was considered unlikely within the 2 hour postdose interval where the second peak occurred. This assumption is supported by previous results which have shown that peaks due to trans-resveratrol enterohepatic recycling appeared on average approximately 4 hours after intra-gastric administration in rats (Marier et al. 2002).

Population PK parameters for trans-resveratrol in rabbits after multiple doses of 12.5% trans-resveratrol cream was characterized by a high clearance (CL/F) of 21.5 L/h, a long absorption half-life of 7.06 hours and a short elimination half-life of

7.76 minutes. Population results for the 19% trans-resveratrol formulation was similar, and was characterized by a high clearance (CL/F) of 75.3 L/h, an absorption half-life of 4.26 hours and an elimination half-life of 5.11 minutes. The pharmacokinetics thus appeared to be characterized by "flip-flop" kinetics where the absorption half-life is much longer than the elimination half-life (Rowland and Tozer 1992). The slope of the terminal phase of the concentration-time profile is representative of drug absorption rather than elimination half-life of the drug. The occurrence of elevated plasma concentrations on Days 14 and 28 compared to those observed after a single application of cream on Day 1 may therefore have been a reflection of a long process of cutaneous and systemic trans-resveratrol absorption after multiple daily doses. The fifth and last dose of trans-resveratrol cream on Day 13 or Day 27 was approximately 16 hours prior to the collection of the predose samples on Days 14 and 28. This 16-hour interval between doses corresponds to an estimated 123 to 188 elimination half-lives based on the estimated $T_{½kel}$ of 7.76 and 5.11 minutes for the 12.5% and 19.0% formulations, respectively. From the literature, *in vivo* data obtained after topical application of norephedrine, for example, appeared to be characterized by "flip-flop" kinetics (Riegelman 1974; Roberts et al. 1999). Absorption of drug through the skin was described using first-order kinetics with a first-order constant rate of absorption ($time^{-1}$).

Cutaneous absorption processes of trans-resveratrol through the skin after topical application is currently unknown, however, delays in absorption may represent changes in permeability due to solute-skin interactions, such as possible binding of the active compound to the stratum corneum or subcutaneous fat, where it may be slowly released into the capillaries for days or weeks after initial application

(Riviere 1993; Smith et al. 1999). A portion of the compound that binds to the stratum corneum may be lost by exfoliation, hence never penetrate the skin layers to the capillaries. In addition to capillary uptake, alternate processes of cutaneous removal may occur such as uptake into the lymphatic circulation and deep dermal penetration, by-passing the capillaries and cutaneous metabolism. Partitioning effects and diffusion of the solute through heterogeneous membranes defining the layers of the skin may also result in time-dependent changes in permeability (Roberts et al. 1999). Improved percutaneous absorption is generally observed with increased stratum corneum reservoir concentration. These possible solute-skin interactions and skin reservoir effects may be complex and cannot be accounted for in detail using a simplified first-order pharmacokinetic model.

The elimination rate constants may not have been robustly assessed in this study; however, a short plasma elimination half-life was not unexpected based on data in the literature. An elimination half-life of approximately 15 minutes had been reported after i.v. administration of trans-resveratrol in rabbits (Asensi et al. 2002) and also after p.o. administration in rats (Juan et al. 2002) and 3.74 minutes after i.p. administration in rats (Zhu et al. 2000).

The high variability inherent to the concentration data and PK results may have occurred predominantly from inter-animal variability, as well as the variability in the application of the dose and skin treatments such as shaving the site. In addition, washing with soap between doses from Day 10 to Day 28 might have affected the barrier integrity of the stratum corneum. Variability was also introduced by using extrapolated concentrations between the LLOQ and LLOD which may have increased the probability of fitting analytical "noise".

Potential Factors Affecting Bioavailability

1. Amount of Cream Applied Per Dose

Low and mid dose groups (4 mg and 20 mg of 12.5% trans-resveratrol cream) gave the highest dose-normalized Cmax, possibly due to factors such as the thickness of the applied layer, evaporation effects, amount of trans-resveratrol in the cream and hydration effects. The amount of cream applied to the site can affect drug delivery (Flynn 1993). Evaporation of excipients begins immediately after topical application, condensing the concentration of trans-resveratrol and enhancing its penetration through the skin surface. When 4 mg and 20 mg of 12.5% trans-resveratrol cream and 66 mg of 19% trans-resveratrol cream was applied to a 4 cm^2 area, the thickness of the layers varied at each dose level. The molecules at the top of the thickest layer of cream (66 mg) must diffuse across a greater distance to reach the skin surface, potentially delaying cutaneous penetration. The rate of condensed trans-resveratrol formation is greatest in the thinnest layer (4 mg), since the ratio of evaporated material to trans-resveratrol is small; however, a residue may form quickly, impeding drug delivery.

2. Washing Solution between Applications

In the preclinical rabbit study, washing the site between dose applications was important in order to remove any residue which may impede cutaneous absorption of a subsequent dose. Water was initially deemed insufficient to remove this residue and a soap solution was introduced on Day 10. Washing the skin with a soap solution, however, could have extracted lipids from the stratum corneum, which decreases its barrier properties (Pugh 1999). A relative bioavailability factor had

been added to the final population PK model in order to account for possible differences in systemic absorption due to this change in procedure but the overall quality of fit did not improve (results not shown).

3. Concentration of Applied Solute

Increasing the concentration of applied solute to the skin appears to increase percutaneous penetration up to a certain point where a plateau may be reached (Rougier et al. 1999). Percutaneous penetration of trans-resveratrol after application of the 19% formulation may have been increased compared to the 12.5% cream; however, corresponding increased plasma concentrations were not observed. Precipitation of the active compound out of the excipient can halt drug delivery. The 19% trans-resveratrol cream contains 6.5% less water than the 12.5% cream. This, combined with a higher concentration of active compound, may increase the risk of trans-resveratrol precipitation out of solution, making drug delivery unsustainable. In addition, skin hydration generally appears to enhance drug permeation especially across the stratum corneum barrier, which favors the higher water content in the 12.5% formulation.

Ideally, a trans-resveratrol cream formulated to treat HSV infections should produce an effective trans-resveratrol concentration in the basal epidermis layer with minimal systemic exposure. Plasma trans-resveratrol concentrations observed after topical application of both creams confirm that the compound was able to diffuse through the skin layers and reach the basal epidermis, where active HSV replication occurs, and beyond. Although trans-resveratrol plasma concentrations were measured after topical application of both cream formulations, it remains impossible to determine whether an effective trans-resveratrol concentration was reached in the

epithelial cells at the basal epidermis. In addition, the 12.5% trans-resveratrol cream at a lower trans-resveratrol dose per application than the 19% formulation was shown to be effective against HSV lesion formation *in vivo* in mice, which may favor the former formulation (Docherty at al. 2004).

Allometric Scaling

Allometric scaling from the current *in vivo* preclinical data presented in this thesis and data obtained from the literature (Asensi et al. 2002) was used to extrapolate the apparent total clearance of oral and topical trans-resveratrol administration in humans. A one-compartment model with multiple absorption peaks best described the PK of trans-resveratrol after topical application while a two-compartment model best described the mouse, rat and rabbit mean trans-resveratrol concentrations reported in the Asensi study. The apparent bi-exponential elimination exhibited by the mean concentration profiles could be attributed to the high variability (CV 30-50%) observed for the mean concentrations at the end of the profiles (Asensi et al. 2002). Individual concentrations were not provided, however, possible BLQ values at the end of the profiles could have accounted for this high variability and also resulted in lower mean concentrations at the end of the profiles. In addition, a 1-compartment model best described the PK of trans-resveratrol in humans (n = 3) after a single oral 1000 mg trans-resveratrol dose (Marier 2003).

A good coefficient of correlation (R^2 = 0.9985) was observed for oral clearance in mouse, rat and rabbit. The high apparent oral clearance predicted in humans (17031 L/h) may be due to the 1-hour plasma collection period used in the preclinical study following i.g. administration of 20 mg/kg trans-resveratrol solution

(Asensi et al. 2002). In a previous study conducted in healthy human volunteers, an apparent clearance of approximately 1800 L/h was calculated using noncompartmental methods after a 1000 mg trans-resveratrol oral dose (unpublished data). In that study, plasma was collected over 24 hours; however, all profiles were near or below the limit of quantitation at 12 hours post dose. Individual profiles showed evidence of multiple absorption peaks and/or enterohepatic circulation due to decreases and subsequent increases in concentrations as late as 4 hours after the initial absorption peak. Population compartmental analysis of these results also predicted extensive trans-resveratrol oral clearance of 2835 L/h and approximately 33% of the drug undergoing enterohepatic circulation (EHC) (Marier 2003). In support of possible EHC in humans, trans-Resveratrol EHC has been clearly demonstrated in rats by use of a linked-rat model (Marier et al. 2002). As a result, the elimination of trans-resveratrol may not have been adequately characterized within the short 1-hour sampling period in the previous work by Asensi et al. since enterohepatic circulation would have occurred later.

We estimated that a 300 mg trans-resveratrol dose in humans (12.5% trans-resveratrol cream) would be required to produce the estimated effective plasma AUC of 0.573 μg·h/L for the treatment of HSV. Simulations in humans of a 300 mg trans-resveratrol topical dose applied every 2 hours for 5 applications predicted plasma concentrations up to a maximum of approximately 0.025 μg/mL (25 μg/L), a concentration well below the *in vitro* effective range of 25 – 50 μg/mL (Docherty et al. 1999). Similarly, the concentration range of 0.000191 – 0.000382 μg/mL estimated to have been reached in the mouse efficacy study (Docherty et al. 2004)

was also well below the *in vitro* effective range. The authors of this preclinical study note however, that the needle burr used to induce HSV infection may have disrupted the barrier function of the stratum corneum potentially increasing treatment efficacy compared to models with an intact stratum corneum. Nevertheless, at trans-resveratrol plasma concentrations below the *in vitro* effective range, topical application of 12.5% trans-resveratrol cream appeared to inhibit HSV replication in mice *in vivo*.

Considering that plasma concentrations are in equilibrium at the biophase, the predicted high trans-resveratrol topical dose of approximately 300 mg in humans may support the current hypothesis in the literature that suggests a possible pharmacological activity of trans-resveratrol conjugates. In another study, simulations in humans were performed to predict effective steady state plasma concentrations after oral administrations of trans-resveratrol (Marier 2003). Potentially toxic oral doses of trans-resveratrol (1500 mg/kg b.i.d.) were required to produce average plasma concentrations (Cave) of trans-resveratrol within the target *in vitro* effective range of 10 – 20 µmol/L (2.28 – 4.56 µg/mL). However, assuming that both trans-resveratrol and its glucuronide are pharmacologically active, simulations predicted that oral doses of only 25 mg/kg b.i.d. would be effective.

That trans-resveratrol conjugates may be pharmacologically active has also been proposed in other publications reporting low trans-resveratrol bioavailability and extensive metabolism (Kuhnle et al. 2000; Asensi et al. 2002). Examples of other drug conjugates that exhibit pharmacological activity include the morphine-3-glucuronide (M3G) and morphine-6-glucuronide (M6G) morphine conjugates (Hasselstrom and Sawe 1993). Interestingly, antioxidant properties have been

reported for the conjugates of quercetin, a flavonoid found in foods such as fruits, vegetables, nuts and seeds (Morand et al. 1998; Manach et al. 1998). Although metabolic activity in the skin appears to be much lower than the activity in the intestine or liver, drug conjugation in human skin has been reported (Hotchkiss 1998). In addition, topical application of 8 and 16 μmol resveratrol to shaved dorsal skin of female mice induced UDP-glucuronosyltransferase in the epidermis layer by 150 and 100%, respectively (Szaefer et al. 2004). These results support the hypothesis that resveratrol may undergo glucuronidation in the skin prior to reaching the systemic circulation.

The topical 300 mg trans-resveratrol dose in humans reported above was estimated with the assumption that the systemic availability of mouse and human skin is similar. It should be noted that species-specific percutaneous absorption has been reported in the literature (Wester and Maibach 1993). In one study, human skin appeared to be a more efficient barrier than mouse skin for a topically applied tea polyphenol EGCG (Dvorakova et al. 1999). The skin of common laboratory animals such as rats and rabbits tends to be more permeable than human skin, while the weanling pig and monkey appear to be better predictors of human *in vivo* absorption. Species-specific dermal conjugation reactions *in vitro* have also been reported for the pesticide propoxur, where glucuronides and sulfates were detected in equal amounts in pig skin, whereas only sulfates were detected in human skin, and glucuronides were predominant in rabbit skin with only minor amounts of sulfides (van de Sandt et al. 1993). Human predictions scaled from preclinical percutaneous absorption data may therefore have limited applicability due to species-specific dermal characteristics.

Future Work

trans-Resveratrol's path through the skin layers prior to capillary absorption is currently unknown. For toxicology purposes, measurement in plasma is important; however, measurement in the skin, especially human skin, may be more informative to predict local skin efficacy. Nevertheless, the current results from this study confirmed that trans-resveratrol did cross the skin layers and reached the basal epidermis where active HSV replication occurs. Radiolabelled methods that characterize the permeability barrier of the human skin *in vivo* or track the radiolabeled compound through the skin might be helpful to establish the fate of trans-resveratrol after topical application (Pirot et al. 1997). This would allow the determination of the possible binding affinity of trans-Resveratrol to the stratum corneum. The quantity of active compound penetrating through the skin layers may be predicted from the amount measured in the stratum corneum reservoir approximately 30 minutes after topical application (Rougier et al. 1983) Rougier suggests that the relationship between the amount in the stratum corneum and percutaneous absorption is defined by a parabolic curve that may be independent of animal species (Rougier et al. 1999). If a measurable quantity of compound is present in the stratum corneum after application, tape-stripping methods used to quantify these amounts may circumvent the use of radiolabeled compounds in humans. Tape-stripping involves multiple site applications of an adhesive tape followed by abrupt removal. If the stratum corneum is the rate-limiting step in absorption, quantification of drug concentration in this barrier may provide an

estimate of the rate and extent of absorption to the lower skin layers (Naik et al. 1999).

Measurement of the stratum corneum reservoir may also be a good predictor of efficacy, as was possibly demonstrated for the topical drug iododeoxyuridine against HSV lesion reduction *in vivo* in the guinea pig (Sheth et al. 1987). Sheth et al. appeared to show that dosing frequency had an effect on the iodedeoxyuridine stratum corneum concentration and corresponding efficacy. A plateau in efficacy and stratum corneum AUC was reached at a dosing frequency of 3 applications per day. Thus, cutaneous pharmacokinetics can possibly examine factors that influence topical bioavailability of various trans-resveratrol formulations by predicting the concentration of trans-resveratrol in the target basal epidermis. Another method estimated concentrations of free drug at the target site (C*) based on experimentally determined *in vitro* flux data and topical *in vivo* efficacy (Mehta et al. 1997). A good correlation was observed between predicted C* and *in vivo* antiviral efficacy of acyclovir against HSV-1 infections using a hairless mouse model (Patel et al. 1996).

Allometric scaling results in this thesis may support the current hypothesis suggesting that trans-resveratrol conjugates may play an active role in producing desired pharmacological effects. Thus, determining a possible pharmacological role of trans-resveratrol conjugates against HSV replication may be a valid hypothesis for future research.

CHAPTER 5: CONCLUSION

As far as we know, this is the first study that characterized the PK of trans-resveratrol after multiple topical applications in rabbits. The 12.5% trans-resveratrol formulation appeared to be more bioavailable than the 19.0% formulation. A population PK model characterized by two absorption peaks was developed and population PK parameters were determined for two trans-resveratrol cream formulations. The PK results presented in this thesis may support current development of an effective topical trans-resveratrol cream against HSV infection.

A topical dose in humans was predicted using allometric scaling and simulations predicted possible trans-resveratrol plasma concentrations after multiple topical applications of 12.5% trans-resveratrol cream. Predicted plasma concentrations were lower than effective *in vitro* concentrations, supporting research into estimating trans-resveratrol's concentration in the local target area in the skin as well as investigating possible activity of trans-resveratrol sulfate and glucuronide conjugates against HSV replication.

REFERENCES

Adrian, M., P. Jeandet, et al. (2000). "Stilbene content of mature Vitis vinifera berries in response to UV-C elicitation." J Agric Food Chem **48**(12): 6103-5.

Andlauer, W., J. Kolb, et al. (2000). "Assessment of resveratrol bioavailability in the perfused small intestine of the rat." Drugs Exp Clin Res **26**(2): 47-55.

Asensi, M., I. Medina, et al. (2002). "Inhibition of cancer growth by resveratrol is related to its low bioavailability." Free Radic Biol Med **33**(3): 387-98.

Aumont, V., S. Krisa, et al. (2001). "Regioselective and stereospecific glucuronidation of trans- and cis-resveratrol in human." Arch Biochem Biophys **393**(2): 281-9.

Beal, S. L. (2001). "Ways to fit a PK model with some data below the quantification limit." J Pharmacokinet Pharmacodyn **28**(5): 481-504.

Bhat, K. P. and J. M. Pezzuto (2002). "Cancer chemopreventive activity of resveratrol." Ann N Y Acad Sci **957**: 210-29.

Bourne, H. R. and M. von Zastrow (2004). Drug Receptors and Pharmacodynamics. Basic & Clinical Pharmacology, Ninth edition. B. G. Katzung, McGraw-Hill Companies, Inc., U.S.A.

Boxenbaum, H. (1992). "Pharmacokinetics: philosophy of modeling." Drug Metab Rev **24**(1): 89-120.

Burns, J., T. Yokota, et al. (2002). "Plant foods and herbal sources of resveratrol." J Agric Food Chem **50**(11): 3337-40.

Calabrese, E. J. (1984). "Suitability of animal models for predictive toxicology: theoretical and practical considerations." Drug Metab Rev **15**(3): 505-23.

Ciolino, H. P., P. J. Daschner, et al. (1998). "Resveratrol inhibits transcription of CYP1A1 in vitro by preventing activation of the aryl hydrocarbon receptor." Cancer Res **58**(24): 5707-12.

Collins, D. and A. Forrest (1995). IT2S User's Guide. Buffalo, State University of New York at Buffalo.

D'Argenio, D. Z. and A. Schumitzky (1998). Adapt II Pharmacokinetic/Pharmacodynamic Systems Analysis Software, User's Guide to Release 4. Los Angeles, Biomedical Simulations Resource.

Davies, B. and T. Morris (1993). "Physiological parameters in laboratory animals and humans." Pharm Res **10**(7): 1093-5.

De Clercq, E. (2004). "Antiviral drugs in current clinical use." J Clin Virol **30**(2): 115-33.

Docherty, J. J. and M. Chopan (1974). "The latent herpes simplex virus." Bacteriol Rev **38**(4): 337-55.

Docherty, J. J., M. M. Fu, et al. (1999). "Resveratrol inhibition of herpes simplex virus replication." Antiviral Res **43**(3): 145-55.

Docherty, J. J., J. S. Smith, et al. (2004). "Effect of topically applied resveratrol on cutaneous herpes simplex virus infections in hairless mice." Antiviral Res **61**(1): 19-26.

Donnelly, L. E., R. Newton, et al. (2004). "Anti-inflammatory effects of resveratrol in lung epithelial cells: molecular mechanisms." Am J Physiol Lung Cell Mol Physiol **287**(4): L774-83.

Dulik, D. M. and C. Fenselau (1987). "Species-dependent glucuronidation of drugs by immobilized rabbit, rhesus monkey, and human UDP-glucuronyltransferases." Drug Metab Dispos **15**(4): 473-7.

Dvorakova, K., R. T. Dorr, et al. (1999). "Pharmacokinetics of the green tea derivative, EGCG, by the topical route of administration in mouse and human skin." Cancer Chemother Pharmacol **43**(4): 331-5.

Evers, D. L., X. Wang, et al. (2004). "3,4',5-Trihydroxy-trans-stilbene (resveratrol) inhibits human cytomegalovirus replication and virus-induced cellular signaling." Antiviral Res **63**(2): 85-95.

Fleming, D. T., G. M. McQuillan, et al. (1997). "Herpes simplex virus type 2 in the United States, 1976 to 1994." N Engl J Med **337**(16): 1105-11.

Flynn, G. L. (1993). General Introduction and Conceptual Differentiation of Topical and Transdermal Drug Delivery Systems. Topical Drug Bioavailability, Bioequivalence, and Penetration. V. P. Shah and H. I. Maibach. New York, Pennum Press.

Foster, D. M. (2001). Chapter 8: Noncompartmental vs. Compartmental Approaches to Pharmacokinetic Analysis. Principles of Clinical Pharmacology. J. Arthur J. Atkinson. San Diego, Academic Press.

Frankel, E. N., A. L. Waterhouse, et al. (1993). "Inhibition of human LDL oxidation by resveratrol." Lancet **341**(8852): 1103-4.

Gabrielsson, J. and D. Weiner (2000). Pharmacokinetic/pharmacodynamic data analysis: concepts and applications. Stockholm, Sweden, Apotekarsocieteten.

Gabrielsson, J, Jukso, WJ and Alari, L. (2000) "Modeling of Dose-Response-Time Data: Four Examples of Estimating the Turnover Parameters and Generating Kinetic Functions from Response Profiles." Biopharmaceutics & Drug Disposition **21**(2):41-52.

Gehm, B. D., J. M. McAndrews, et al. (1997). "Resveratrol, a polyphenolic compound found in grapes and wine, is an agonist for the estrogen receptor." Proc Natl Acad Sci U S A **94**(25): 14138-43.

Gescher, A. J. and W. P. Steward (2003). "Relationship between mechanisms, bioavailibility, and preclinical chemopreventive efficacy of resveratrol: a conundrum." Cancer Epidemiol Biomarkers Prev **12**(10): 953-7.

Gibaldi, M. and D. Perrier, Eds. (1982). Pharmacokinetics, Second Edition, Revised and Expanded. Drugs and the Pharmaceutical Sciences. Volume 15. New York, Marcel Dekker, Inc.

Gould, S. J. (1979). "One Standard Lifespan." New Scientist **8**: 388-389.

Hammond-Kosack, K. E. and J. D. Jones (1996). "Resistance gene-dependent plant defense responses." Plant Cell **8**(10): 1773-91.

Hasselstrom, J. and J. Sawe (1993). "Morphine pharmacokinetics and metabolism in humans. Enterohepatic cycling and relative contribution of metabolites to active opioid concentrations." Clin Pharmacokinet **24**(4): 344-54.

Hattori, R., H. Otani, et al. (2002). "Pharmacological preconditioning with resveratrol: role of nitric oxide." Am J Physiol Heart Circ Physiol **282**(6): H1988-95.

Heredia, A., C. Davis, et al. (2000). "Synergistic inhibition of HIV-1 in activated and resting peripheral blood mononuclear cells, monocyte-derived macrophages, and selected drug-resistant isolates with nucleoside analogues combined with a natural product, resveratrol." J Acquir Immune Defic Syndr **25**(3): 246-55.

Hotchkiss, S. (1998). Dermal Metabolism. Dermal Absorption and Toxicity Assessment. M. Roberts and K. Walters. New York, Marcel Dekker, Inc. **91:** 43-101.

Howitz, K. T., K. J. Bitterman, et al. (2003). "Small molecule activators of sirtuins extend Saccharomyces cerevisiae lifespan." Nature **425**(6954): 191-6.

Huang, C., W. Y. Ma, et al. (1999). "Resveratrol suppresses cell transformation and induces apoptosis through a p53-dependent pathway." Carcinogenesis **20**(2): 237-42.

Jang, M., L. Cai, et al. (1997). "Cancer chemopreventive activity of resveratrol, a natural product derived from grapes." Science **275**(5297): 218-20.

Jelliffe, R., A. Schumitzky, et al. (2002). Population Pharmacokinetic and Pharmacodynamic Modeling, USC Laboratory of Applied Pharmacokinetics, www.lapk.org/pubsinfo/pdf/POP-CHAP-4new.pdf.

Jelliffe, R., A. Schumitzky, et al. (2000). "Population pharmacokinetics/pharmacodynamics modeling: parametric and nonparametric methods." Ther Drug Monit **22**(3): 354-65.

Jenkins, F. J. and S. L. Turner (1996). "Herpes simplex virus: a tool for neuroscientists." Front Biosci **1**: d241-7.

Juan, E. M., J. Buenafuente, et al. (2002). "Plasmatic levels of trans-resveratrol in rats." Food Research International **35**: 195-199.

Juan, M. E., E. Gonzalez-Pons, et al. (2005). "trans-Resveratrol, a Natural Antioxidant from Grapes, Increases Sperm Output in Healthy Rats." J Nutr **135**(4): 757-60.

Kuhnle, G., J. P. Spencer, et al. (2000). "Resveratrol is absorbed in the small intestine as resveratrol glucuronide." Biochem Biophys Res Commun **272**(1): 212-7.

LeBlanc, P.-P. (1997). Chapitre II - Outils et concepts de la biopharmacie et de la pharmacocinétique. Traité de Biopharmacie et Pharmacocinétique. Montréal, Éditions Vigot et Les Presses de L'université de Montréal, 3ème édition.

Manach, C., Morand, C. et al.(1998) "Quercetin is recovered in human plasma as conjugated derivatives which retain antioxidant properties." FEBS Letters **426**:331-336

Marier, J. (2003). Nouvelles approches en pharmacocinétique et pharmacodynamie de population: Application à des médicaments commercialisés et en voie de commercialisation. Thèse de doctorat. Montréal, Université de Montréal.

Marier, J. F., P. Vachon, et al. (2002). "Metabolism and disposition of resveratrol in rats: extent of absorption, glucuronidation, and enterohepatic recirculation evidenced by a linked-rat model." J Pharmacol Exp Ther **302**(1): 369-73.

Mehta, S. C., M. I. Afouna, et al. (1997). "Relationship of skin target site free drug concentration (C*) to the in vivo efficacy: an extensive evaluation of the predictive value of the C* concept using acyclovir as a model drug." J Pharm Sci **86**(7): 797-801.

Meng, X., P. Maliakal, et al. (2004). "Urinary and plasma levels of resveratrol and quercetin in humans, mice, and rats after ingestion of pure compounds and grape juice." J Agric Food Chem **52**(4): 935-42.

Morand, C. and Crespy, V. et al. (1998) "Plasma metabolites of quercetin and their antioxidant properties." Am J Physiol. **275** : 212-219.

Naik, A., Y. N. Kalia, et al. (1999). Characterization of Molecular Transport Across Human Stratum Corneum In Vivo. Percutaneous Absorption, Drugs-Cosmetics-Mechanisms-Methodology. R. L. Bronaugh and H. I. Maibach. 3rd Edition, Revised and Expanded, New York, Marcel Dekker, Inc. **97**.

NDA (2002). "Zovirax CS® (acyclovir) Topical Cream 5% active, Prescribing Information, NDA 21-478." www.fda.gov/cder/foi/nda.

Pace-Asciak, C. R., S. Hahn, et al. (1995). "The red wine phenolics trans-resveratrol and quercetin block human platelet aggregation and eicosanoid synthesis: implications for protection against coronary heart disease." Clin Chim Acta **235**(2): 207-19.

Park, J. W., Y. J. Choi, et al. (2001). "Chemopreventive agent resveratrol, a natural product derived from grapes, reversibly inhibits progression through S and G2 phases of the cell cycle in U937 cells." Cancer Lett **163**(1): 43-9.

Parker, A. and S. Montrowl (2004). "Neonatal Herpes Infection: A Review." NBIN **4**(1): 62-69; www.medscape.com.

Patel, P. J., A. H. Ghanem, et al. (1996). "Correlation of in vivo topical efficacies with in vitro predictions using acyclovir formulations in the treatment of cutaneous HSV-1 infections in hairless mice: an evaluation of the predictive value of the C* concept." Antiviral Res **29**(2-3): 279-86.

Phoenix Automated Statistics & Tabulation (Phast), MDS Pharma Services (formerly Phoenix International Life Sciences) Scientific Software, version 2.3-001, Saint-Laurent (Montreal), Quebec, 1999

Pirot, F., Y. N. Kalia, et al. (1997). "Characterization of the permeability barrier of human skin in vivo." Proc Natl Acad Sci U S A **94**(4): 1562-7.

Potter, G. A., L. H. Patterson, et al. (2002). "The cancer preventative agent resveratrol is converted to the anticancer agent piceatannol by the cytochrome P450 enzyme CYP1B1." Br J Cancer **86**(5): 774-8.

Pugh, W. J. (1999). Relationship Between H-Bonding of Penetrants to Stratum Corneum Lipids and Diffusion. Percutaneous Absorption, Drugs-Cosmetics-Mechanisms-Methodology. R. L. Bronaugh and H. I. Maibach. 3rd Edition, Revised and Expanded, New York, Marcel Dekker, Inc. **97**.

Qureshi, S. A., M. Jiang, et al. (1998). "In vitro evaluation of percutaneous absorption of an acyclovir product using intact and tape-stripped human skin." J Pharm Pharm Sci **1**(3): 102-7.

Riegelman, S. (1974). "Pharmacokinetics. Pharmacokinetic factors affecting epidermal penetration and percutaneous adsorption." Clin Pharmacol Ther **16**(5 Part 2): 873-83.

Riviere, J. (1993). Biological Factors in Absorption and Permeation. Skin Permeation Fundamental and Application. J. Zatz. Wheaton, Allured Publishing Corp.

Roberts, M. S., Y. G. Anissimov, et al. (1999). Mathematical Models in Percutaneous Absorption. Percutaneous Absorption, Drugs-Cosmetics-Mechanisms-Methodology. R. L. Bronaugh and H. I. Maibach. 3rd Edition, Revised and Expanded, New York, Marcel Dekker, Inc. **97**.

Rougier, A., D. Dupuis, et al. (1999). Stripping Method for Measuring Percutaneous Absorption In Vivo. Percutaneous Absorption, Drugs-Cosmetics-Mechanisms-Methodology. R. L. Bronaugh and H. I. Maibach. 3rd Edition, Revised and Expanded, New York, Marcel Dekker, Inc. **97**.

Rougier, A., D. Dupuis, et al. (1983). "In vivo correlation between stratum corneum reservoir function and percutaneous absorption." J Invest Dermatol **81**(3): 275-8.

Rowland , M and Tozer, TN (1992) Clinical Pharmacokinetics, Concepts and Applications, 3rd edition, Lippincott Williams & Wilkins.

Shargel, L. and A. Yu (1999). Applied Biopharmaceutics and Pharmacokinetics. 4th edition, Stamford, Appleton & Lange.

Sheiner, L. and S. Beal (1980). NONMEM Users Guide, parts I & II. Technical Report, Division of Clinical Pharmacology. San Francisco, University of California.

Sheiner, L. B. and S. L. Beal (1983). "Evaluation of methods for estimating population pharmacokinetic parameters. III. Monoexponential model: routine clinical pharmacokinetic data." J Pharmacokinet Biopharm **11**(3): 303-19.

Sheth, N. V., M. B. McKeough, et al. (1987). "Measurement of the stratum corneum drug reservoir to predict the therapeutic efficacy of topical iododeoxyuridine for herpes simplex virus infection." J Invest Dermatol **89**(6): 598-602.

Smith, E. W., C. Surber, et al. (1999). Topical Dermatological Vehicles; A Holistic Approach. Percutaneous Absorption, Drugs-Cosmetics-Mechanisms-Methodology. R. L. Bronaugh and H. I. Maibach. 3rd Edition, Revised and Expanded, New York, Marcel Dekker, Inc. **97**.

Szaefer, H., M. Cichocki, et al. (2004). "Alteration in phase I and II enzyme activities and polycyclic aromatic hydrocarbons-DNA adduct formation by plant phenolics in mouse epidermis." Nutr Cancer **48**(1): 70-7.

van de Sandt, J. J., A. A. Rutten, et al. (1993). "Species-specific cutaneous biotransformation of the pesticide propoxur during percutaneous absorption in vitro." Toxicol Appl Pharmacol **123**(1): 144-50.

Vitrac, X., A. Desmouliere, et al. (2003). "Distribution of [14C]-trans-resveratrol, a cancer chemopreventive polyphenol, in mouse tissues after oral administration." Life Sci **72**(20): 2219-33.

Walle, T., F. Hsieh, et al. (2004). "High absorption but very low bioavailability of oral resveratrol in humans." Drug Metab Dispos **32**(12): 1377-82.

Wester, R. C. and H. I. Maibach (1993). Chapter 18: Animal Models for Percutaneous Absorption. Topical Drug Bioavailability, Bioequivalence, and Penetration. V. P. a. M. Shah, H.I. New York, Plenum Press.

White, D. and F. Fenner (1994). Medical Virology, 4th Edition. San Diego, U.S.A., Academic Press Limited.

WHO (2001). Report of a WHO/UNAIDS/LSHTM Workshop. Herpes Simplex Virus Type 2 Programmatic and Research Priorities in Developing Countries. London, Copyright © World Health Organization and the Joint United Nations Programme on HIV/AIDS (2001) www.who.int/docstore/hiv/herpes_meeting/004.htm.

Williams, A. (2003). Transdermal and Topical Drug Delivery. London, Pharmaceutical Press.

Yu, C., Y. G. Shin, et al. (2002). "Human, rat, and mouse metabolism of resveratrol." Pharm Res **19**(12): 1907-14.

Yu, C., Y. G. Shin, et al. (2003). "Liquid chromatography/tandem mass spectrometric determination of inhibition of human cytochrome P450 isozymes by resveratrol and resveratrol-3-sulfate." Rapid Commun Mass Spectrom **17**(4): 307-13.

Zhu, Y., T. Huang, et al. (2000). "Liquid chromatography with multichannel electrochemical detection for the determination of trans-resveratrol in rat blood utilizing an automated blood sampling device." J Chromatogr B Biomed Sci Appl **740**(1): 129-33.

APPENDIX I

Appendix I – Table 1: Individual Compartmental PK Parameters for the Final Model in Adapt II®

	Rabbit ID	alpha	ka	Vc/F	kel	lag1	delay1	lag28	delay28	int	slope	int2	slope2	ECV	AIC	SCHWARZ	R2[Y(1)]	R2[Y(2)]
Formulation I	1	1.01	0.00	1.3	9.0	0.61	0.50	0.11	1.2	3E-11	3E-13	3E-02	1E+00	-20.2	-16.5	-32.1		
	2	0.17	0.23	5.9	1.9	0.23	0.62	0.33	2.9	7E-02	2E-03	2E-12	6E-07	-14.2	-4.3	-20.0		
	3	0.00	0.03	16.4	0.6	0.04	1.43	0.01	4.2	5E-12	2E-12	5E-01	1E+00	-15.3	-6.6	-13.9	0.663	
	4	0.46	0.16	1.5	3.5	0.03	0.65	0.10	0.4	2E-07	3E-08	6E-02	4E-01	-7.5	8.9	-1.9	1.000	
	5	3.14	0.16	2.2	4.6	0.00	0.09	0.20	0.1	1E-06	6E-08	1E-01	3E-01	-9.0	5.9	-4.9	1.000	
	6	0.45	0.15	5.3	2.5	0.17	0.36	0.23	0.5	2E-01	3E-01	8E-08	1E-08	-28.9	-33.9	-44.7	1.000	
	7	0.40	0.05	7.2	1.8	0.04	0.46	0.09	6.8	4E-02	2E-01	6E-07	2E-06	0.0	24.0	19.3	0.759	
	8	0.66	0.07	13.0	6.1	0.51	0.47	0.00	1.2	2E-08	7E-09	4E-01	2E-02	-16.2	-8.4	-19.2	1.000	
	9	0.61	0.17	2.5	9.1	0.28	0.75	0.06	0.0	3E-09	2E-08	5E-02	6E-01	-4.2	15.6	8.3	0.453	
	10	0.25	0.15	3.7	10.8	0.04	0.01	0.02	0.0	8E-02	4E-01	4E-05	6E-01	10.3	44.6	37.2	1.000	1
	11	0.33	0.15	9.1	3.4	0.06	0.50	0.14	0.0	1E-01	1E+00	4E-11	8E-13	-12.1	-0.3	-7.6	0.459	
	12	0.08	0.14	0.3	14.3	0.02	4.58	0.37	0.2	3E-01	6E-05	2E-07	2E-08	-14.1	-4.1	-6.6	1.000	
Formulation II	13	0.06	0.24	4.6	12.9	0.00	0.50	2.80	1.4	4E-02	3E-01	4E-02	4E-02	6.8	37.6	32.9	1.000	0.587
	14	0.00	0.34	1.3	9.2	0.01	0.65	1.24	1.1	3E-01	1E+00	3E-05	3E-04	-5.7	12.6	7.9	1.000	1
	15	0.37	0.10	19.1	29.2	0.21	0.15	0.26	1.0	5E-01	3E+00	4E-04	3E-01	7.8	39.7	35.0	0.047	
	16	0.23	0.23	34.8	1.6	0.10	0.87	0.72	2.3	4E-07	9E-09	2E-02	5E-01	-20.3	-16.7	-24.1	1.000	1
	17	1.12	0.17	32.0	5.0	0.02	1.52	1.52	2.5	2E-01	9E-01	2E-13	3E-12	-13.8	-3.6	-11.0	0.933	
	18	0.18	0.31	11.9	2.9	0.06	1.97	0.63	4.7	2E-06	2E-09	2E-01	5E-02	-25.1	-26.3	-37.1	1.000	
	19	0.16	0.15	7.4	14.0	0.26	5.03	0.00	0.0	3E-01	8E-01	2E-04	4E-01	34.1	92.2	96.9	0.299	0.420
	20	0.17	0.18	5.7	22.6	0.23	3.99	0.18	0.0	9E-02	4E-01	1E-01	3E-01	18.6	61.2	63.6	0.872	0.001
	21	0.49	0.12	24.0	13.6	0.11	0.60	1.25	1.2	6E-02	1E+00	4E-01	4E-06	14.7	53.5	58.2	0.662	0.579
	22	1.01	0.08	1.1	261.9	0.37	10.50	1.47	1.6	2E-01	2E-01	1E-03	3E-01	18.6	61.3	67.1	0.759	0.088
	23	0.14	0.12	2.3	43.5	0.01	1.98	0.96	0.4	1E+00	2E-01	1E-01	2E-01	17.9	59.8	62.1	0.777	0.858
	24	2.06	0.02	5.5	27.0	0.22	0.81	1.07	1.5	1E+00	6E-01	3E-03	8E-02	28.2	80.5	87.3	0.071	0.971

Appendix I - Table 1 cont'd

	alpha	ka	Vc/F	kel	lag1	delay1	lag28	delay28	int	slope	int2	slope2	ECV	AIC	SCHWARZ	R2[Y(1)]	R2[Y(2)]
Mean	0.564	0.146	9.08	21.30	0.152	1.625	0.574	1.47	0.200	0.432	0.080	0.265	-2.07	19.86	14.69	0.7616	0.6504
SD	0.7188	0.0841	9.658	52.312	0.1658	2.3417	0.6907	1.718	0.3164	0.7001	0.1333	0.3303	17.461	34.922	40.654	0.30997	0.38194
CV%	127.5	57.5	106	246	108.9	144.1	120.4	117.2	158.4	162.2	167.3	124.7	-843	176	277	40.7	58.7
Median	0.348	0.147	5.58	9.07	0.0797	0.650	0.245	1.14	0.076	0.179	0.011	0.164	-6.62	10.766	3.01	0.9025	0.7225
n	24	24	24	24	24	24	24	24	24	24	24	24	24	24	24	22	10
Formulation I	*0.25*	*0.2*	*5*	*2*	*0.2*	*0.4*	*0.1*	*0.5*	*0.1*	*0.1*	*0.1*	*0.15*					
Mean	0.629	0.121	5.71	5.64	0.170	0.868	0.139	1.45	0.069	0.161	0.090	0.344	-10.96	2.08	-7.19	0.8334	1.0000
SD	0.8380	0.0683	4.984	4.249	0.2050	1.2197	0.1219	2.126	0.0995	0.3183	0.1555	0.4244	10.042	20.084	22.010	0.23238	.
CV%	133.2	56.3	87	75	120.4	140.5	87.6	146.6	145.0	197.3	172.8	123.5	-92	963	-306	27.9	.
Median	0.422	0.146	4.49	4.04	0.0516	0.501	0.103	0.42	0.022	0.000	0.016	0.177	-13.10	-2.205	-7.14	1	1
n	12	12	12	12	12	12	12	12	12	12	12	12	12	12	12	10	1
Formulation II	*0.1*	*0.3*	*7*	*3*	*0.3*	*1*	*0.8*	*1*	*0.1*	*0.1*	*0.1*	*0.15*					
Mean	0.499	0.171	12.46	36.96	0.134	2.381	1.009	1.48	0.331	0.702	0.069	0.186	6.82	37.64	36.58	0.7017	0.6115
SD	0.6073	0.0937	12.054	71.892	0.1215	2.9545	0.7552	1.284	0.4024	0.8740	0.1129	0.1857	19.086	38.173	43.894	0.36146	0.38359
CV%	121.8	54.8	97	194	90.5	124.1	74.9	86.7	121.6	124.5	162.7	99.7	280	101	120	51.5	62.7
Median	0.204	0.157	6.57	13.82	0.1071	1.196	1.017	1.30	0.182	0.479	0.011	0.164	11.28	46.564	46.61	0.8245	0.587
n	12	12	12	12	12	12	12	12	12	12	12	12	12	12	12	12	9

Appendix I – Schematic Representation of Some of the Rejected Compartmental PK Models

Model Res1k

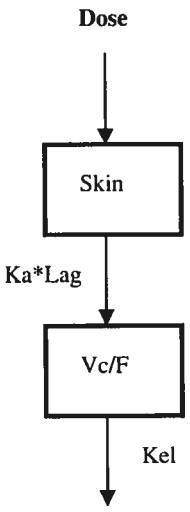

Model Res2k

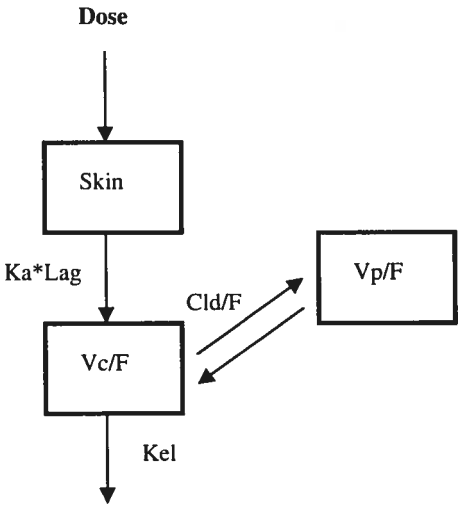

Model Res1a

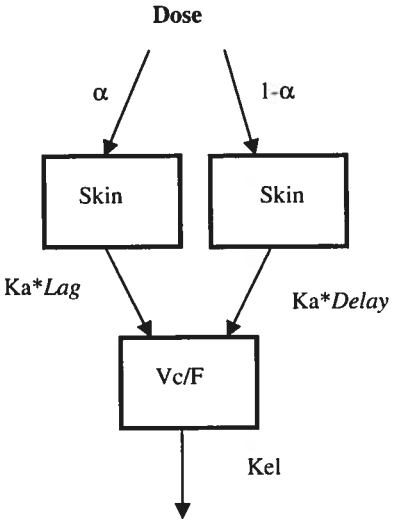

Model Res3d

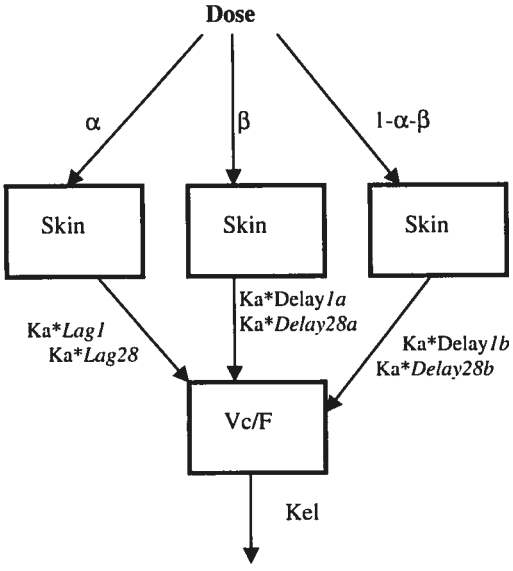

APPENDIX II

Appendix II - Individual Fitted (—) (Final Model) vs observed(•) trans-Resveratrol Concentrations versus Time Following Multiple Topical Administrations of 12.5% trans-Resveratrol Cream for 28 Consecutive Days to 12 Rabbits

Appendix II – 12.5% trans-Resveratrol Cream

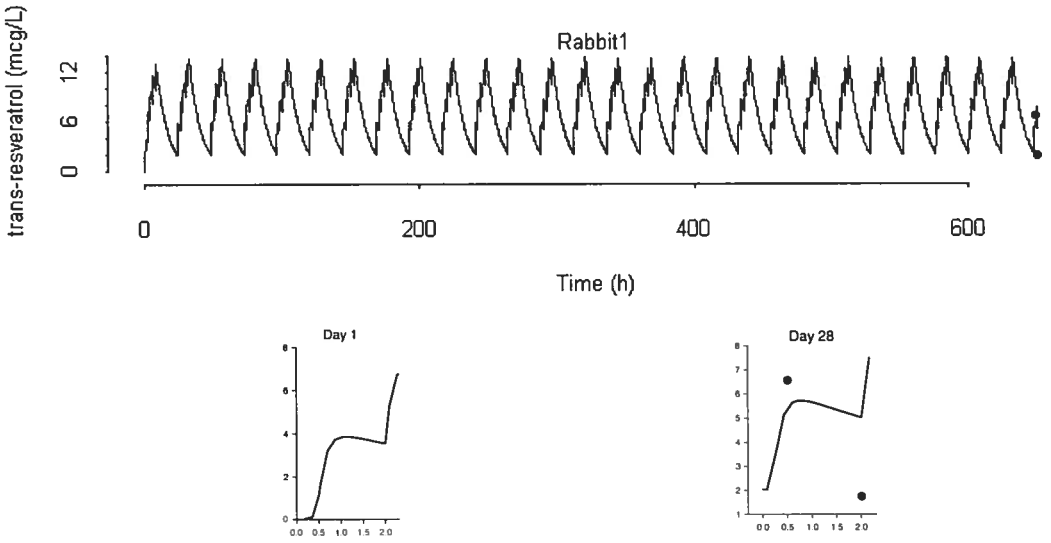

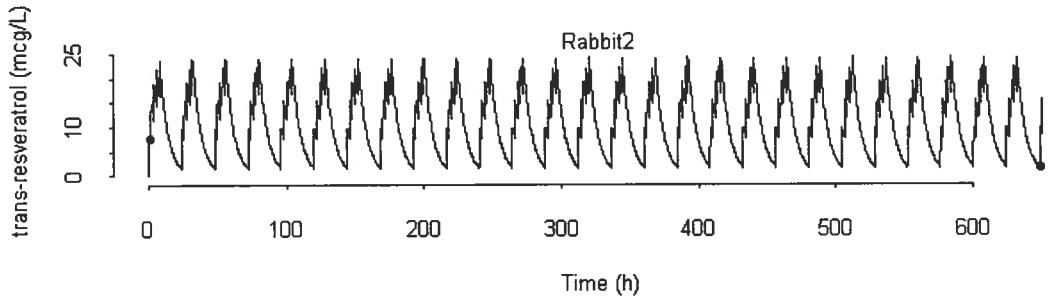

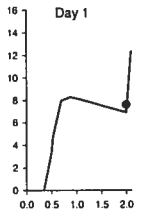

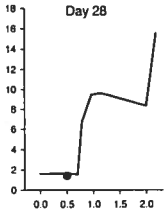

Appendix II – 12.5% trans-Resveratrol Cream

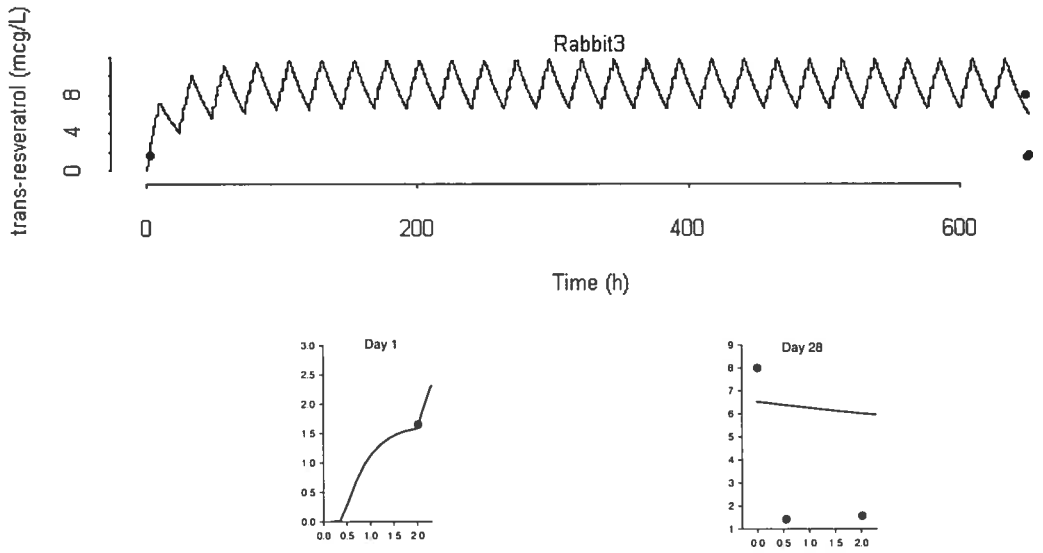

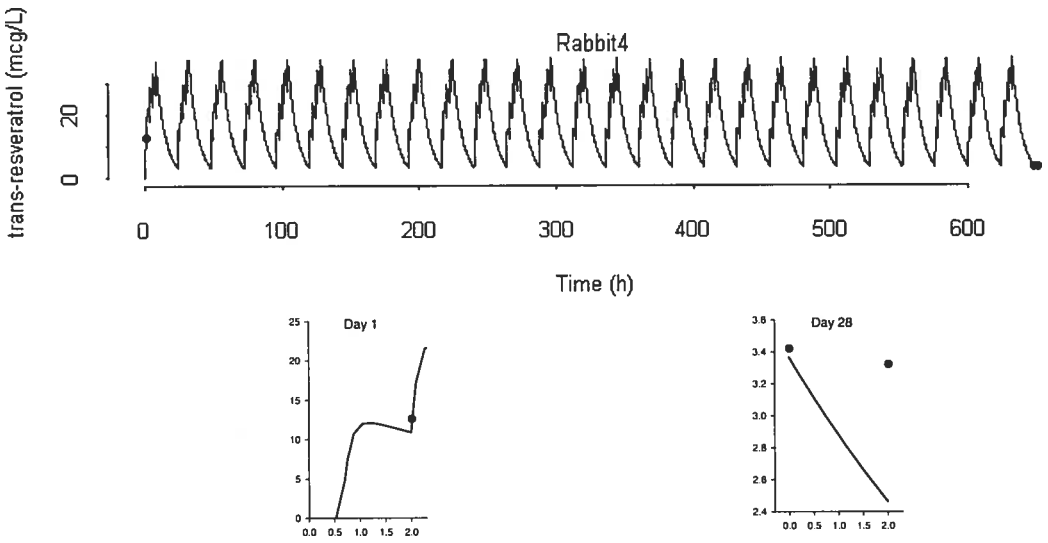

Appendix II – 12.5% trans-Resveratrol Cream

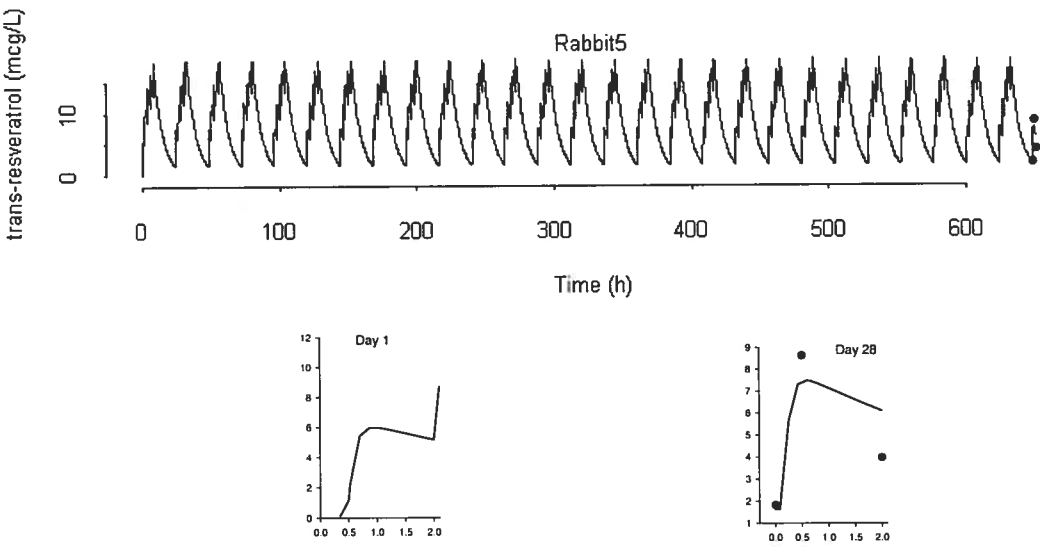

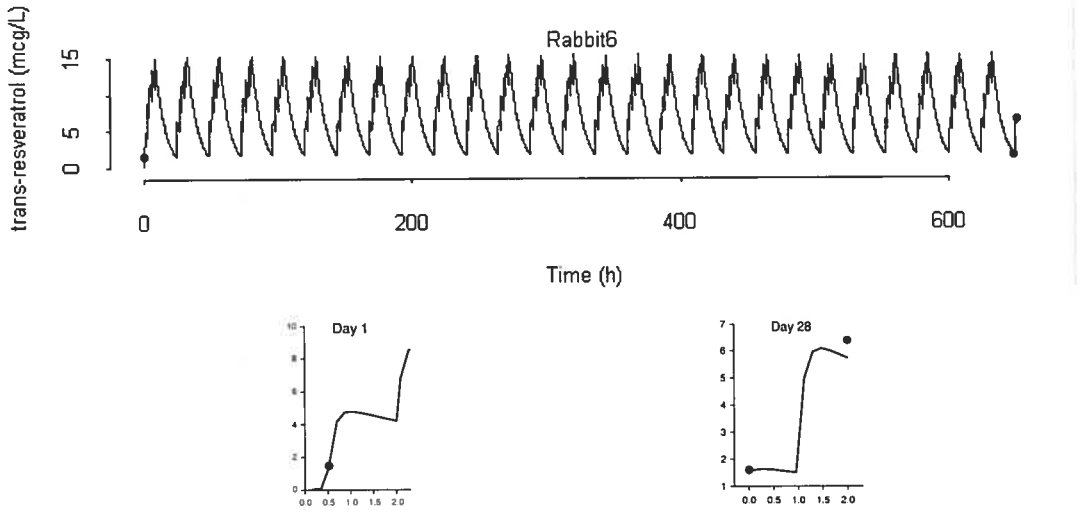

Appendix II – 12.5% trans-Resveratrol Cream

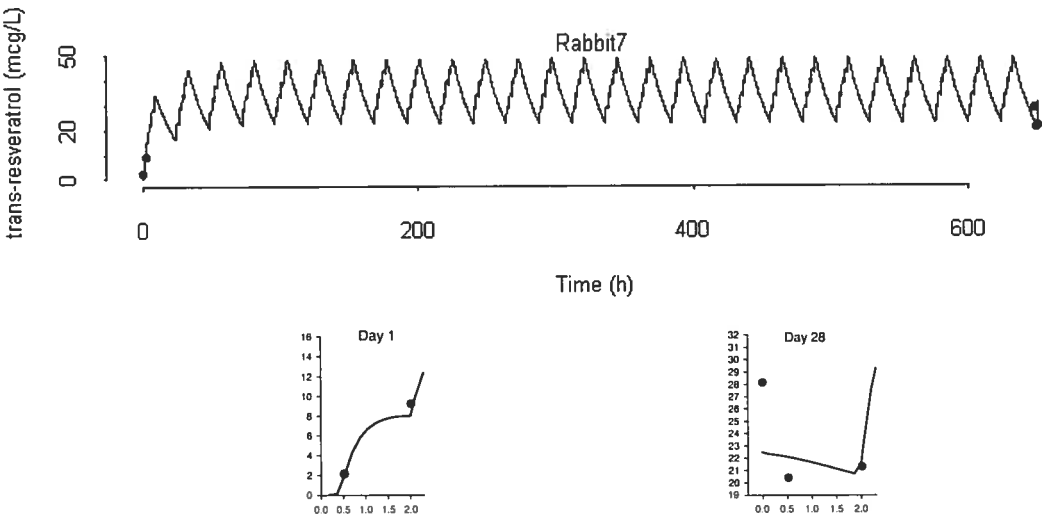

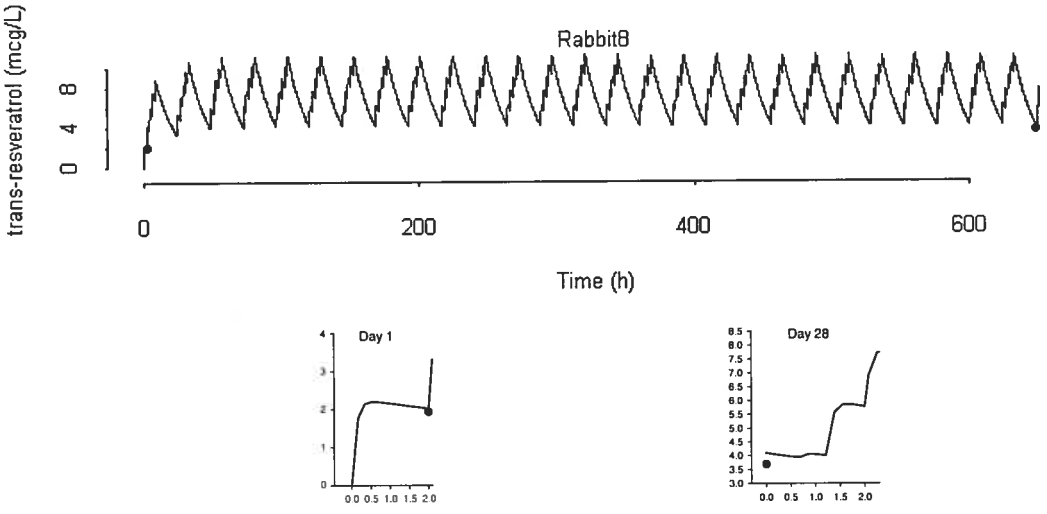

Appendix II – 12.5% trans-Resveratrol Cream

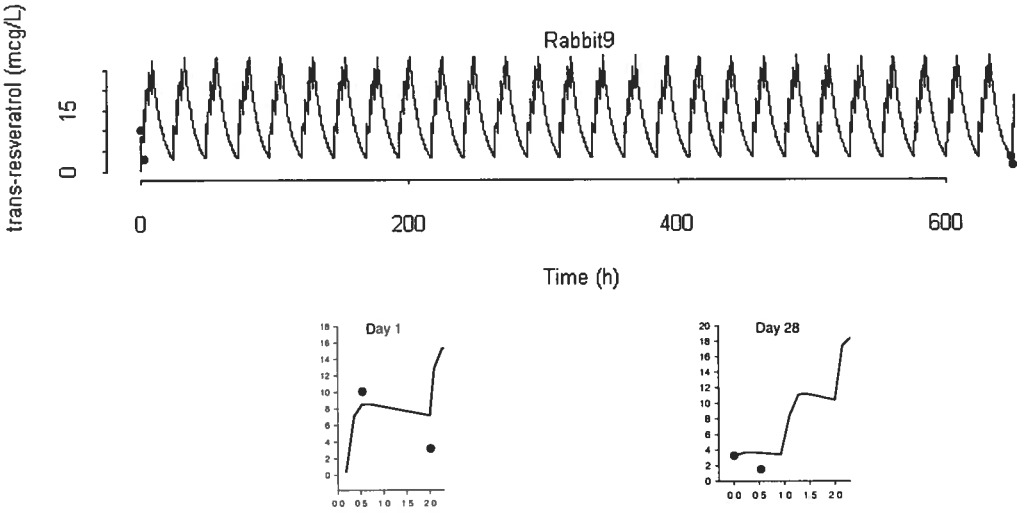

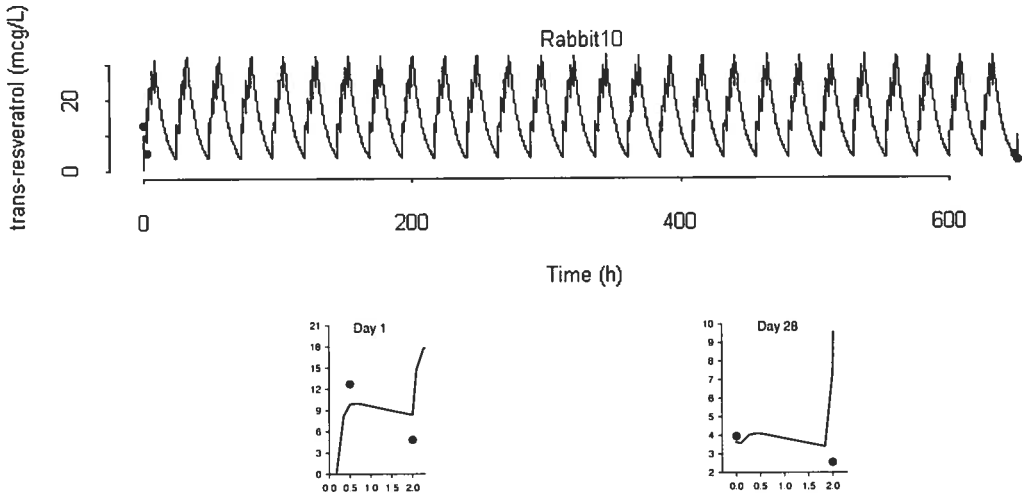

Appendix II – 12.5% trans-Resveratrol Cream

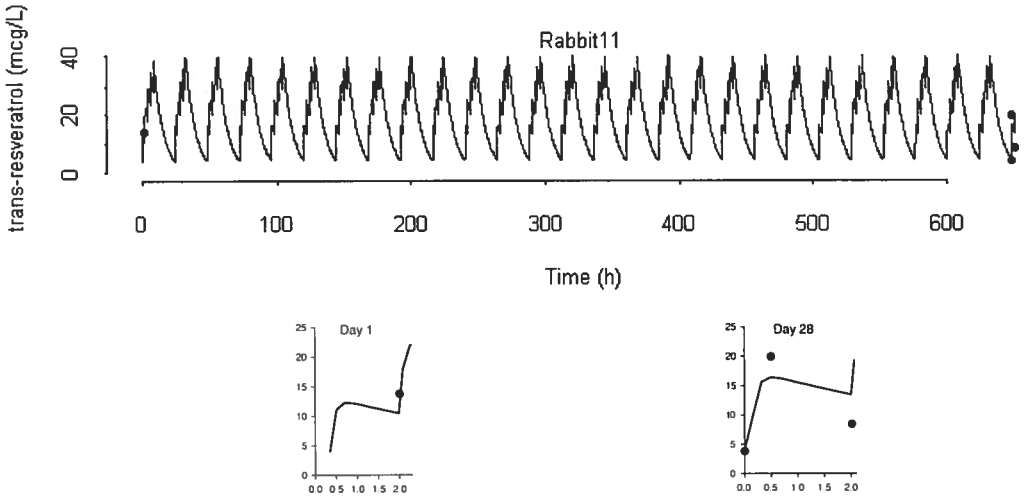

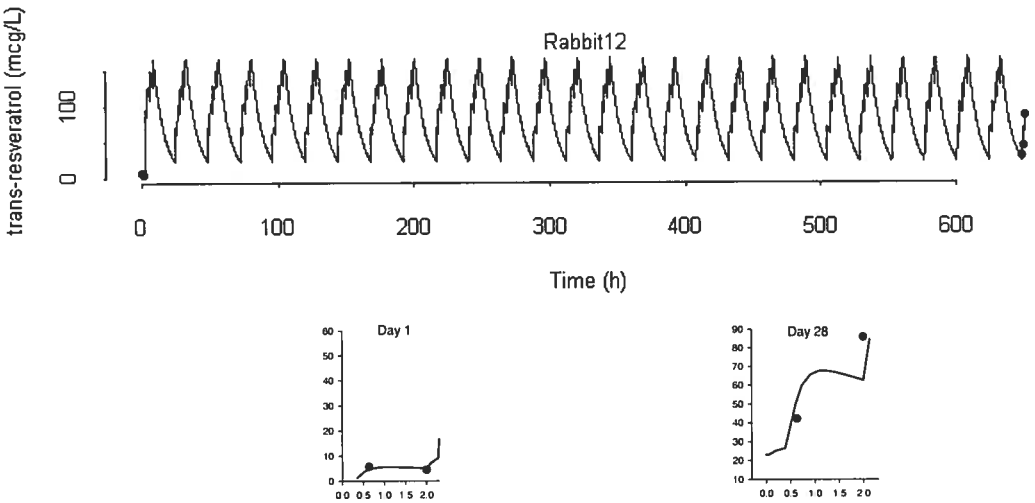

Appendix II - Individual Fitted (—) (Final Model) vs observed(•) trans-Resveratrol Concentrations versus Time Following Multiple Topical Administrations of 19% trans-Resveratrol Cream for 28 Consecutive Days to 12 Rabbits

Appendix II – 19% trans-Resveratrol Cream

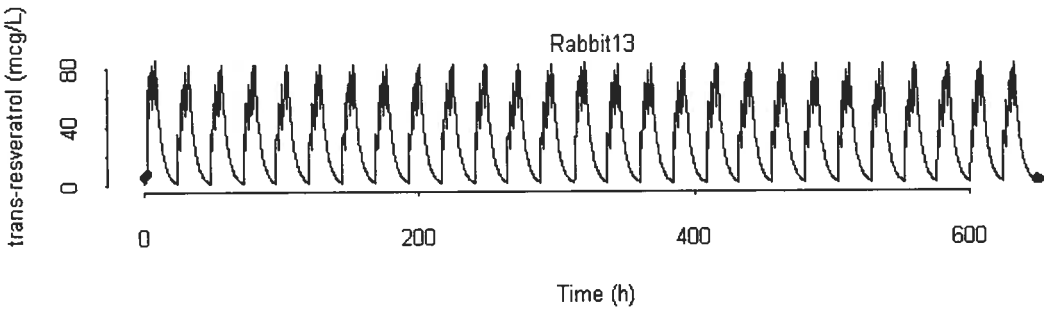

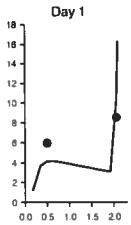

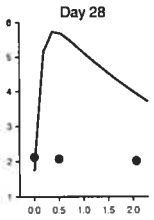

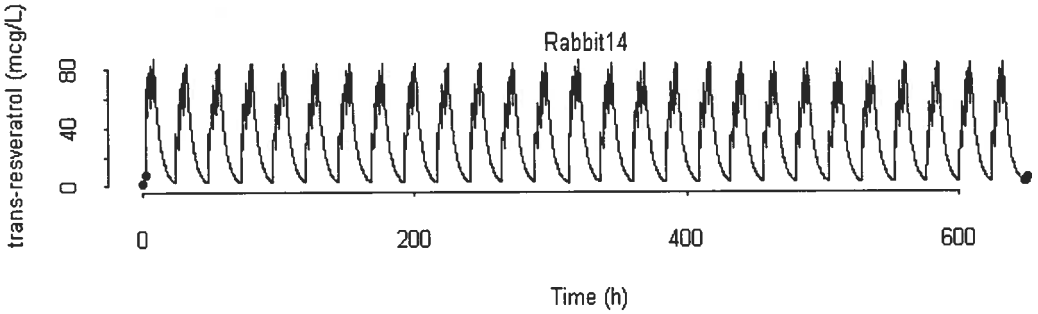

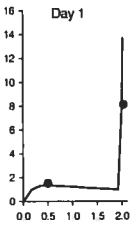

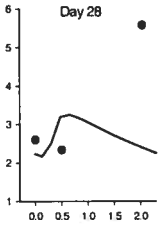

Appendix II – 19% trans-Resveratrol Cream

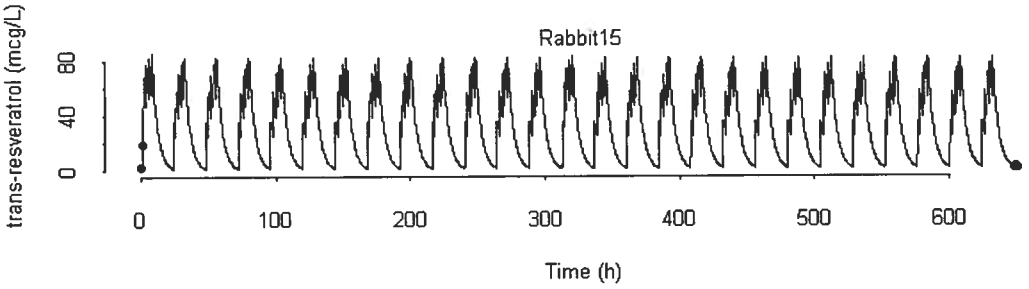

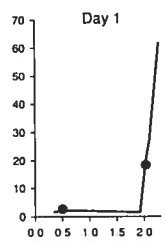

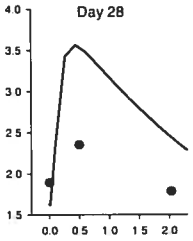

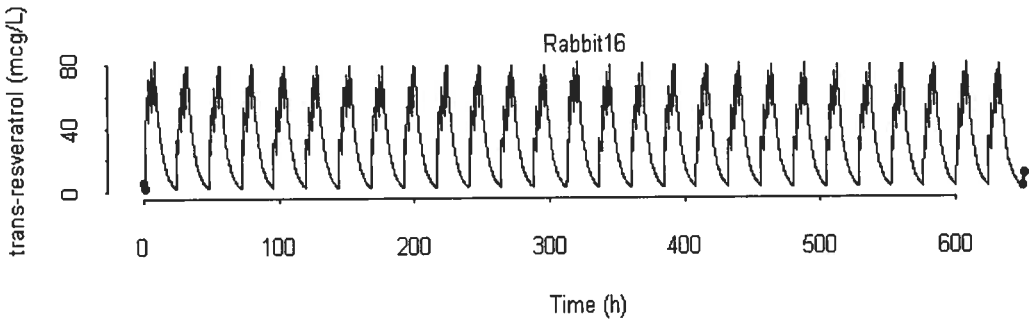

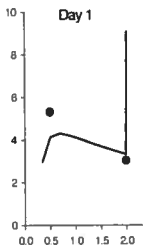

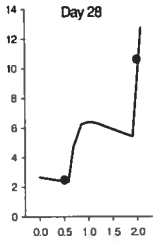

Appendix II – 19% trans-Resveratrol Cream

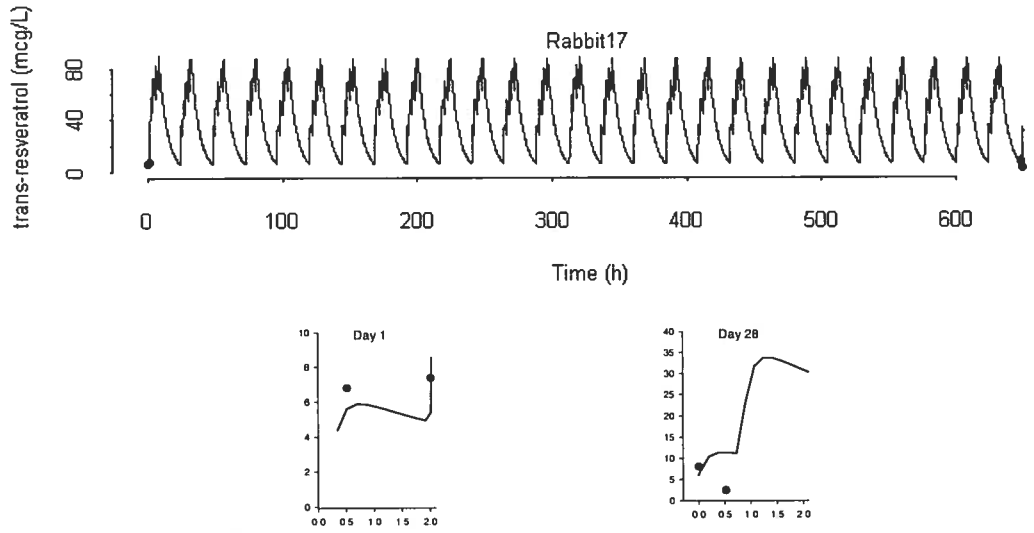

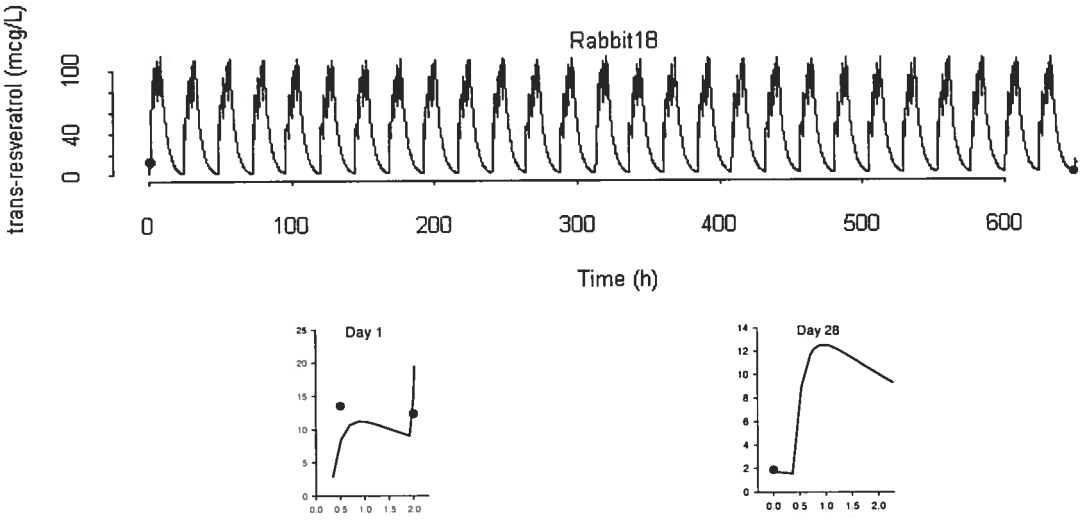

Appendix II – 19% trans-Resveratrol Cream

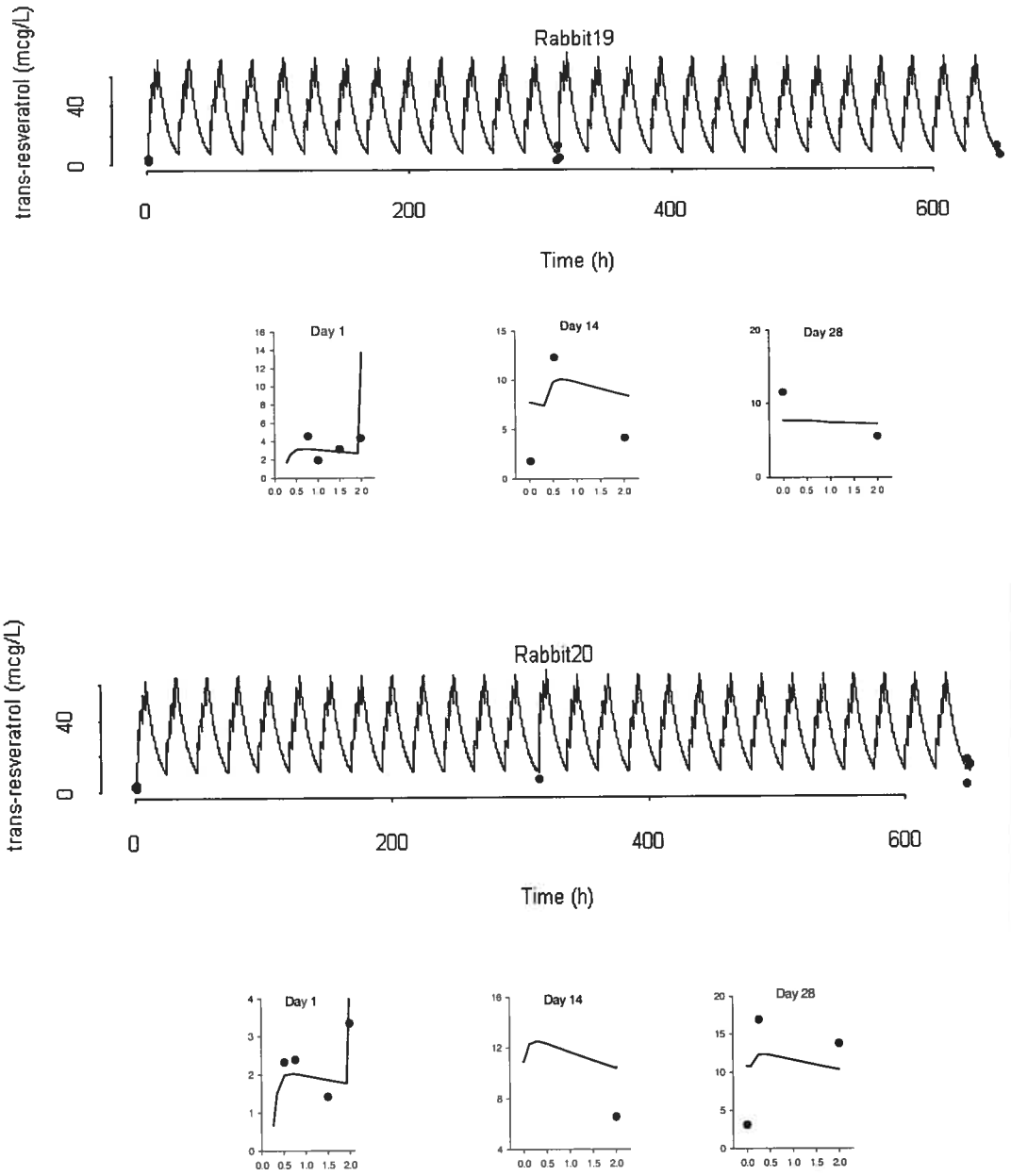

Appendix II – 19% trans-Resveratrol Cream

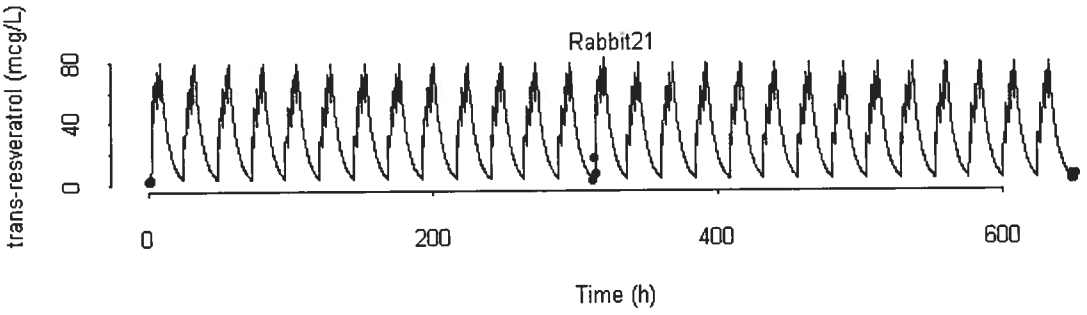

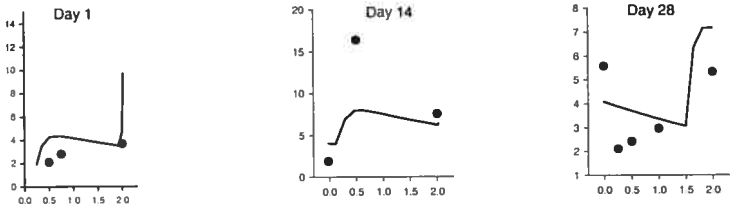

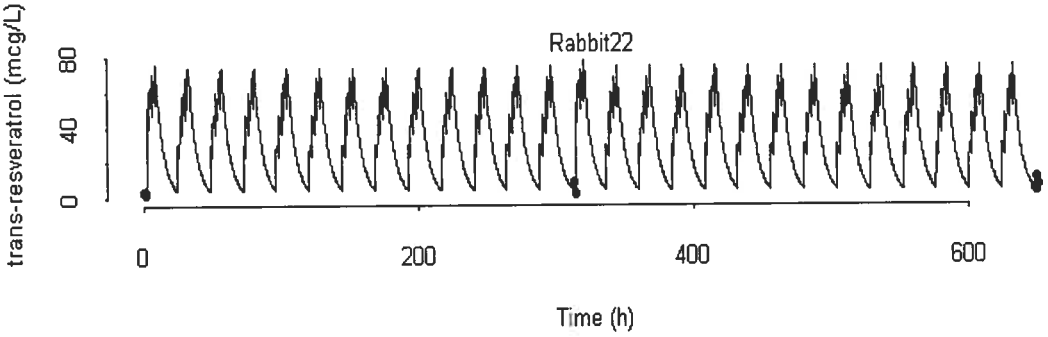

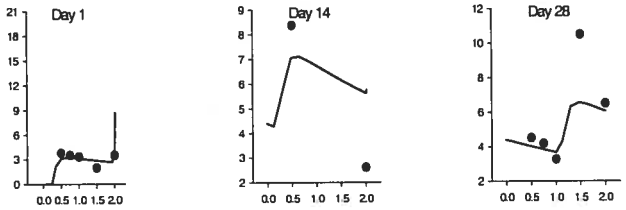

Appendix II – 19% trans-Resveratrol Cream

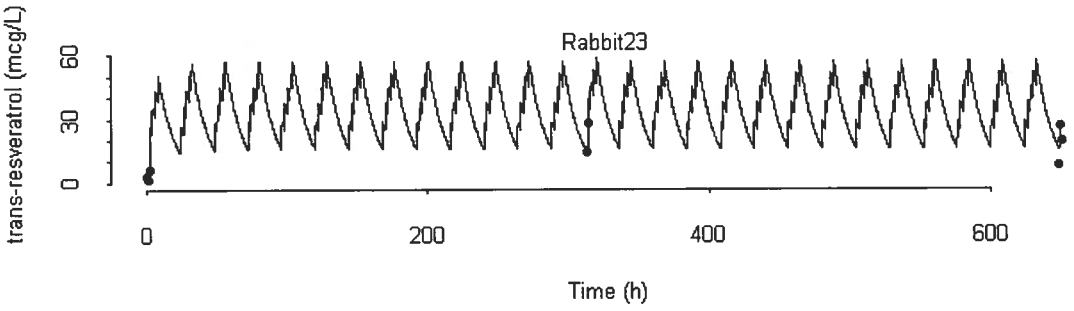

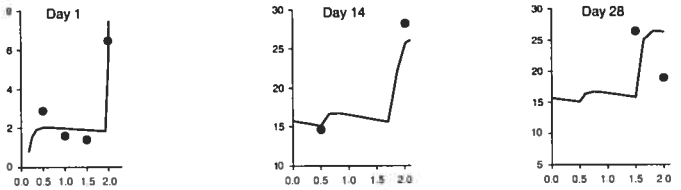

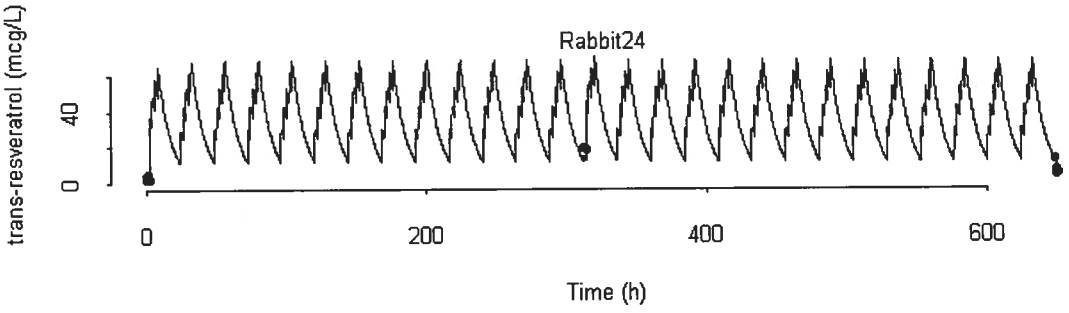

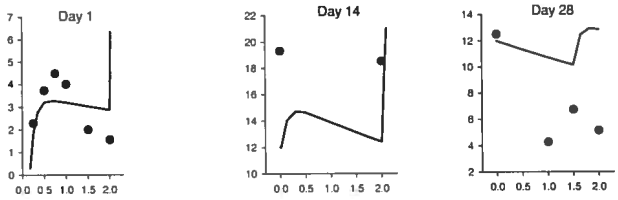

APPENDIX III

Appendix III - Table 1: 12.5% trans-Resveratrol Cream Derived and Calculated Population PK Parameters Obtained Using the Final Model in IT2S®

Parameters/ Rabbit ID	alpha %	Ka (h-1)	Vc/F (L)	Kel (h-1)	lag1 (h)	delay1 (h)	lag28 (h)	delay28 (h)	$T_{½ka}$ (h)	$T_{½kel}$ (min)	CL/F (L/h)
1	0.039	0.123	2.46	5.93	0.14	0.31	0.08	0.10	5.64	0.117	14.6
2	0.016	0.173	0.91	10.8	0.18	0.28	0.14	0.56	4.00	0.064	9.75
3	0.014	0.041	6.58	1.74	0.05	0.36	2.00	2.18	17.1	0.399	11.4
4	0.000	0.156	0.79	7.53	0.21	0.42	0.02	2.00	4.45	0.092	5.91
5	0.035	0.156	1.36	8.91	0.25	0.23	0.13	0.01	4.44	0.078	12.1
6	0.023	0.145	1.76	8.00	0.09	0.39	0.12	0.86	4.77	0.087	14.1
6	0.040	0.052	6.08	2.44	0.11	0.31	0.15	1.80	13.4	0.284	14.9
7	0.099	0.065	7.78	9.07	0.00	0.00	0.67	0.55	10.7	0.076	70.6
9	0.071	0.139	3.44	11.0	0.08	0.13	0.02	0.99	5.00	0.063	38.0
10	0.072	0.141	3.14	10.5	0.13	0.08	0.15	1.80	4.93	0.066	33.1
11	0.073	0.142	2.76	9.74	0.26	0.06	0.06	0.03	4.90	0.071	26.9
12	0.116	0.130	1.36	4.45	0.30	2.00	0.07	0.38	5.35	0.156	6.06
Mean	0.050	0.122	3.202	7.514	0.150	0.382	0.301	0.939	7.057	0.1293	21.457
SD	0.0360	0.0441	2.3644	3.2006	0.0903	0.5278	0.5620	0.8078	4.2738	0.10525	18.5986
CV%	72.3	36.3	73.8	42.6	60.0	138.2	186.7	86.1	60.6	81.4	86.7
Median	0.039	0.140	2.614	8.456	0.136	0.295	0.124	0.709	4.964	0.0822	14.352
n	12	12	12	12	12	12	12	12	12	12	12

Variability:	Residual $Error_1$	Residual $Error_2$
$Intercept_1$: $0.5916x10^{-7}$	21.7%	42.1%
$Slope_1$: 0.2166		
$Intercept_2$: $0.4680x10^{-4}$		
$Slope_2$: 0.4213		

Appendix III - Table 2: 19% trans-Resveratrol Cream Derived and Calculated Population PK Parameters Obtained Using the Final Model in IT2S®

Parameters/ Rabbit ID	alpha %	Ka (h-1)	Vc/F (L)	kel (h-1)	lag1 (h)	delay1 (h)	lag14 (h)	delay14 (h)	lag28 (h)	delay28 (h)	$T_{½ka}$ (h)	$T_{½kel}$ (min)	CL/F (L/h)
13	0.121	0.248	10.2	7.95	0.14	1.90	0.31	0.92	0.01	2.90	2.79	5.23	80.72
14	0.039	0.234	9.48	8.20	0.03	1.94	0.45	0.82	0.26	2.48	2.96	5.07	77.72
15	0.061	0.253	9.79	8.36	0.20	1.75	0.19	0.96	0.05	2.70	2.74	4.97	81.90
16	0.140	0.219	9.72	8.27	0.23	1.77	0.34	0.92	0.60	1.45	3.17	5.03	80.39
17	0.199	0.173	9.96	6.65	0.17	1.84	0.18	0.73	0.00	0.80	4.00	6.26	66.19
18	0.239	0.270	12.2	5.01	0.30	1.67	0.30	0.88	0.37	2.00	2.56	8.29	61.01
19	0.140	0.144	8.38	8.92	0.19	1.76	0.32	2.00	0.50	2.00	4.80	4.66	74.77
20	0.115	0.114	7.12	10.7	0.23	1.75	0.0005	2.50	0.08	2.00	6.09	3.87	76.44
21	0.156	0.190	9.39	8.25	0.19	1.81	0.17	2.00	1.50	2.00	3.64	5.04	77.45
22	0.123	0.182	8.71	9.24	0.25	1.75	0.24	2.00	1.10	1.75	3.82	4.50	80.47
23	0.154	0.083	6.55	11.6	0.13	1.84	0.50	1.30	0.50	1.00	8.37	3.60	75.69
24	0.175	0.112	8.12	8.76	0.16	1.84	0.01	2.00	1.50	2.00	6.18	4.75	71.13
Mean	0.1385	0.1852	9.129	8.492	0.185	1.801	0.251	1.419	0.539	1.924	4.261	5.106	75.324
SD	0.05441	0.06183	1.4903	1.6866	0.0669	0.0742	0.1524	0.6299	0.5474	0.6221	1.7864	1.2071	6.3421
CV%	39.3	33.4	16.3	19.9	36.2	4.12	60.7	44.4	102	32.3	41.9	23.6	8.42
Median	0.1399	0.1860	9.432	8.317	0.188	1.790	0.267	1.129	0.433	2.000	3.728	5.000	76.944
n	12	12	12	12	12	12	12	12	12	12	12	12	12

Variability:	Residual $Error_1$	Residual $Error_2$
$Intercept_1$: $0.528x10^{-9}$	33.8%	34.1%
$Slope_1$: 0.3378		
$Intercept_2$: 0.00196		
$Slope_2$: 0.3410		

APPENDIX IV

Appendix IV – Figure 1: Mean trans-Resveratrol Concentrations (Asensi et al. 2002) Fitted with a Two Compartmental PK Model in Adapt II® after Intra-gastric Administration of 20 mg/kg trans-Resveratrol Solution to Rabbit, Rat and Mouse

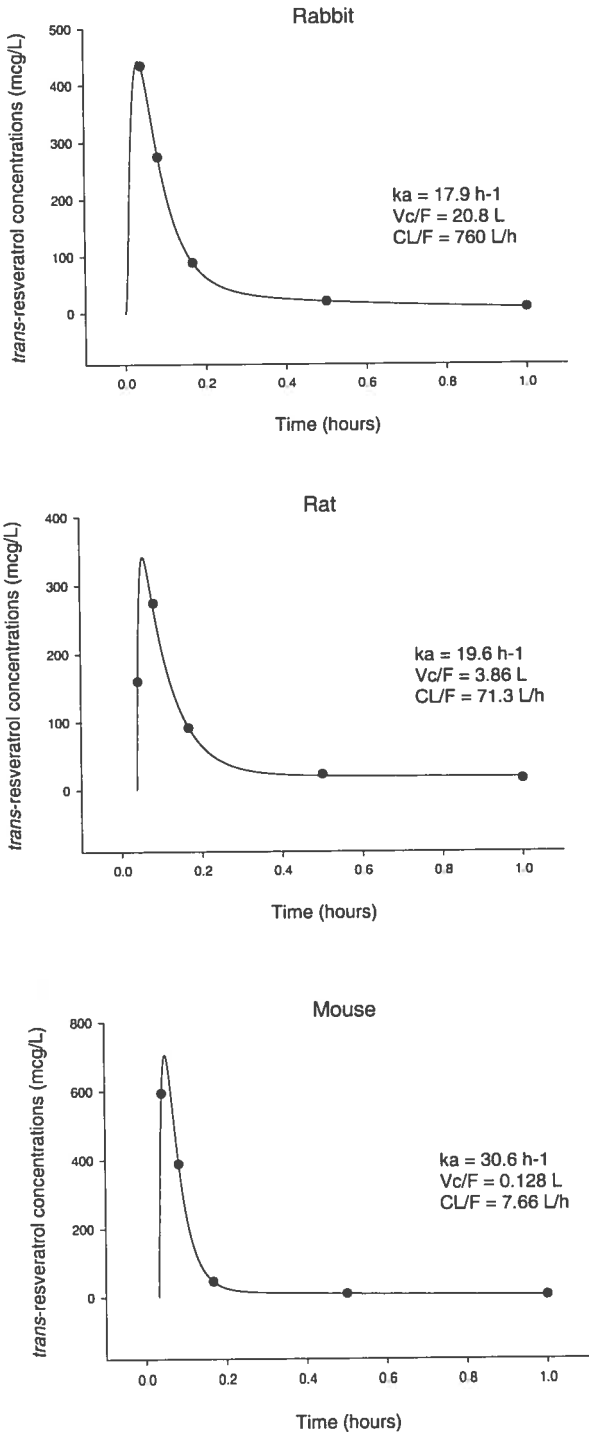

Appendix IV – Figure 2: Allometric Scaling Results for Peripheral PK Parameters Fitted using a Two Compartment Model in Adapt II® for Mouse, Rat, and Rabbit Mean Concentration Data and Extrapolated to Humans

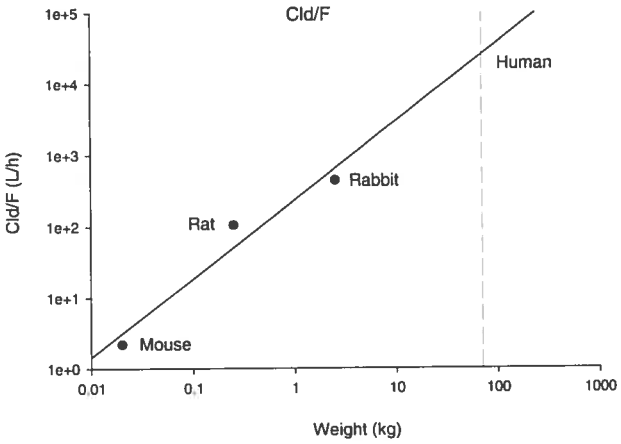

Coefficients:
b[0]=2.3728852742
b[1]=1.1064958652
r^2=0.9468

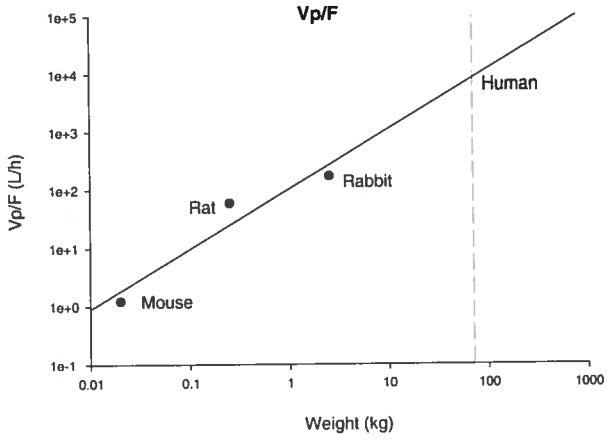

Coefficients:
b[0]=2.0198532253
b[1]=1.0322351215
r^2=0.9184